Reprinted from ANNALS OF PHYSICS
All Rights Reserved by Academic Press, New York and London

Vol. 199, No. 2, May 1, 1990
Printed in Belgium

Nonequilibrium Steady States and Phase Transitions in Driven Diffusive Systems*

P. L. GARRIDO† AND J. MARRO

Departamento de Física Aplicada, Facultad de Ciencias, Universidad de Granada, E-18071-Granada, Spain

AND

R. DICKMAN

Department of Physics and Astronomy, Lehman College, CUNY, Bronx, New York 10468-1589

Received September 13, 1989

We present general analytical solutions of a driven diffusive lattice gas obtained by means of a kinetic cluster-variation approach and other techniques and discuss in detail the method which can be applied to a large class of kinetic systems. In particular, we consider explicitly one- and two-dimensional versions of the model, providing more general results than have been derived previously. Our study reveals relaxation to a rich variety of steady nonequilibrium states, including states which are segregated anisotropically under the action of the external driving force; such states occur, for instance, in the so-called super-ionic-conductor systems under the presence of an external electric field. We also make comparisons with related models and with recent Monte Carlo data.

1. INTRODUCTION

The study of nonequilibrium steady states and phase transitions has recently benefited from the analysis of some novel model systems involving, either explicitly or implicitly, the action of some external agent. Indeed, valuable progress has emerged from the consideration of a fluid under shear [1], particle systems driven by an external electric field and other driven systems [2–11], models with competing dynamics, such as reaction-diffusion [12–14] or the case of several locally competing temperatures [15], spatial gradients of temperature [16], etc.

The present paper is devoted to the study of a driven diffusive system (DDS), which is relevant to so-called fast or super ionic conductors, i.e., solid electrolytes

* Partially supported by the DGICYT, Spain, Project PB85-0062.
† Present address: Department of Mathematics, Hill Center, Rutgers University, New Brunswick, NJ 08903. Supported by NSF Grant DMR86-12369.

0003-4916/90 $7.50

of great technological interest [17–23]. The model system is a lattice gas (equivalently an Ising model) whose particles bear a positive charge, (only) in the sense that they are driven along one of the principal directions of the lattice, under the influence of a uniform external electric field **E**. This field cannot be included in the Hamiltonian, but influences the transition probabilities for the (stochastic) evolution of the system configuration together with the action of a heat reservoir at temperature T which absorbs the heat generated by the particle current. The model also incorporates a parameter, Γ, which governs the rate of transitions in the direction of the field as compared to those perpendicular to it. Such a (particle conserving) hopping dynamics drives the system asymptotically to a (nonequilibrium) steady state, eventually suffering various kinds of instabilities (and metastabilities) which are absent in the equilibrium case, i.e., $E=0$. Similar models were studied before from a rather general point of view [2] and by using Monte Carlo methods for strong fields [2–6]; there are also some solutions [7, 8] in certain limiting conditions (which correspond to having E and $\Gamma \to \infty$) implying mean-field behavior, and field-theoretical treatments under some simplifying hypotheses [9–10].

We present here the solution of the basic model for arbitrary values of $E \in [0, \infty]$ and $\Gamma \in [0, \infty]$ in the case of linear and square lattices. Our method of solution is, essentially, a kinetic version of Kikuchi's cluster variation method [24] for the case of a dynamics proceeding via exchange processes; this allows a series of successive approximations within the philosophy of a mean-field solution. Such a procedure proves most convenient in the present context. It may be applied to many other situations; in fact, a similar method was applied previously to models with spin flip dynamics [16, 25, 26]. Second, mean-field approximations may happen to be more realistic here than in equilibrium [3, 4, 7, 8]. Finally, in addition to allowing for consideration of arbitrary values for E and Γ, the present method may be applied to any kind of interactions between particles, e.g., attractive (ferromagnetic) or repulsive (antiferromagnetic) ones, and to any form of transition probabilities for the hopping dynamics.

Applied to the two-dimensional version of the model, our solution reveals the key feature previously observed in the computer simulations for strong fields [4–6], of anisotropic segregation at low temperatures. That is, there will be coexistence of a homogeneous gas (particle-poor) phase and a homogeneous liquid (particle-rich) phase, the latter forming a single strip, whose characteristic width depends on the particle density n, parallel to the field direction. We thus find a rich and interesting behavior as one varies n, T, E, and Γ (and, eventually, transition probabilities and sign or nature of interactions). The model is interesting even in one dimension where new features emerge.

The paper is organized as follows. Section 2 formulates the model, and Sections 3 and 4 present the description of the general method of solution, including the analysis of the approximations involved. The method is applied in Section 5 to the solution of the one-dimensional model for arbitrary values of n, E, and Γ in the case of both Metropolis and Kawasaki transition probabilities. Sections 6 to 9 deal with two-dimensional versions of the model. Section 7 contains a generalization of

the cases considered previously by van Beijeren and Schulman [7] and by Krug *et al.* [8]. That is, while those studies specifically refer to the limit $\Gamma \to \infty$ and $E \to \infty$, our treatment, which is based on our previous one-dimensional solution and on a Ω-expansion technique, allows, as well, the consideration of finite values for E and the study of the two limits $\Gamma \to \infty$ and 0. The case $\Gamma \to 0$ is considered separately in Section 8. Section 9 follows the kinetic-cluster variation method to solve the two-dimensional model for arbitrary dynamics and values of n, E, and Γ. The solution derived in Section 9 incorporates the existence of a well-defined interface at low temperatures; we discuss with greater detail the case $\Gamma = 1$ which can be compared with Monte Carlo data. Section 10 presents a somewhat different method for finding the critical temperature and other properties by studying the stability of the high temperature phase. Finally, Section 11 summarizes our most important findings.

2. The Model

Let us consider a lattice gas system (equivalently, an Ising spin system) on a simple cubic lattice in d dimensions with configurations $\sigma = \{\sigma_{\mathbf{x}}; \mathbf{x} \in Z^d, \sigma_{\mathbf{x}} = 1, 0\}$, where the two states of the occupation variable, $\sigma_{\mathbf{x}} = 1, 0$, are interpreted, respectively, as having a particle (positive ion) or an empty site at $\mathbf{x}$. The configuration energy is given by

$$H(\boldsymbol{\sigma}) = -4J \sum_{|\mathbf{x}\ \mathbf{y}|=1} \sigma_{\mathbf{x}}\sigma_{\mathbf{y}}, \tag{2.1}$$

where the sum is over nearest neighbor (n.n.) pairs. There is an external uniform electric field, **E**, along one of the principal directions of the lattice which, together with the (stochastic) action of the heat reservoir at temperature T, induces the time evolution of $\boldsymbol{\sigma}$ according to the master equation

$$dP_E(\boldsymbol{\sigma}; t)/dt = \sum_{|\mathbf{x}\ \mathbf{y}|=1} [c_E(\boldsymbol{\sigma}^{\mathbf{x},\mathbf{y}}; \mathbf{x}, \mathbf{y})\, P_E(\boldsymbol{\sigma}^{\mathbf{x},\mathbf{y}}; t) - c_E(\boldsymbol{\sigma}; \mathbf{x}, \mathbf{y})\, P_E(\boldsymbol{\sigma}; t)], \tag{2.2}$$

where $\boldsymbol{\sigma}^{\mathbf{x},\mathbf{y}}$ represents the configuration $\boldsymbol{\sigma}$ with the occupation variables at n.n sites $\mathbf{x}$ and $\mathbf{y}$ interchanged, $P_E(\boldsymbol{\sigma}; t)$ is the probability density of configuration $\boldsymbol{\sigma}$ at time t, and $c_E(\boldsymbol{\sigma}; \mathbf{x}, \mathbf{y})$ is the transition probability per unit time for the interchange, when the system configuration is $\boldsymbol{\sigma}$. The latter will be taken to have the form

$$c_E(\boldsymbol{\sigma}; \mathbf{x}, \mathbf{y}) = \Phi[\beta H(\boldsymbol{\sigma}^{\mathbf{x},\mathbf{y}}) - \beta H(\boldsymbol{\sigma}) - \mathbf{E} \cdot (\mathbf{x} - \mathbf{y})(\sigma_{\mathbf{x}} - \sigma_{\mathbf{y}})] \tag{2.3}$$

with $\beta = 1/k_B T$. This includes most familiar choices as particular cases, e.g., "Metropolis rates,"

$$\Phi(h) = \min[1, e^{-h}], \tag{2.4}$$

and "Kawasaki rates,"

$$\Phi(h) = [1 + e^h]^{-1}, \tag{2.5}$$

One may also mention the choice

$$\Phi(h) = e^{-h/2} \tag{2.6}$$

which has been used in a related nonequilibrium problem [7].

The model defined above involves more or less standard hypotheses and has a number of interesting features: (i) The interaction between ions is assumed to reduce (as a consequence of a collective effect), to an effective short-ranged interaction which may be neglected beyond n.n. positions. (ii) It is assumed as well that there is some justification for the above discrete description and Markovian evolution, i.e., the potential barriers at each lattice site in the modeled material are high enough so that the ions remain static most of the time. (iii) When $E=0$, the family (2.3) of transition probabilities satisfies detailed balance ((2.4) and (2.5) then reduce to the most familiar transition probabilities [27, 28]), so that the system tends asymptotically to the equilibrium Gibbs state with energy $H(\sigma)$ whose nature is well known. In particular, there is a critical temperature T_c ($T_c=0$ for $d=1$, and $T_c>0$ for $d\geqslant 2$) such that there is a unique state for $T\geqslant T_c$ while there is (isotropic) phase segregation for $T<T_c$. (iv) For $E\neq 0$, the steady state, $P_E(\sigma)$, is not an equilibrium state, and it may depend on the choice for the function Φ in Eq. (2.3). The investigation of the nature of this state as one varies several parameters is of primary interest, as it may present both continuous and discontinuous instabilities. (v) The transition probabilities (2.3) satisfy *locally* a detailed balance condition, and make $P_E(\sigma)$ invariant under translations and symmetric under the transformation $E\to -E$ and $\sigma_{\mathbf{x}}\to 1-\sigma_{\mathbf{x}}$ for all $\mathbf{x}$. (vi) One may show that Eqs. (2.1)–(2.3) imply familiar results in equilibrium statistical mechanics, namely the Kubo formulae for bulk diffusivity and electrical conductivity, and that the state of minimum entropy production only agrees with the stationary solution of (2.2) to linear order in E [2]. Further details of the model may be found in Refs. [2–10, 29].

3. Kinetics of Local Clusters

Following the philosophy of Kikuchi's cluster-variation method [24] (see also Refs. [11, 16, 25, 26]), we develop here a procedure to deal with *kinetic* models evolving via interchange processes. The resulting description has a mean-field nature because it rests upon the construction of specific equations for the time evolution of mean local quantities, neglecting long-wavelength fluctuations; such equations may be derived from the master equation, Eq. (2.2), with condition (2.3), under well-defined hypotheses.

The microscopic dynamical functions $A(\sigma)$, which are of interest here for obtaining

macroscopic quantities $\langle A\rangle_t$, only depend in practice on the occupation variables at a relatively small, compact set of lattice sites, say a local domain D. That is, $A(\boldsymbol{\sigma})\equiv A(\boldsymbol{\sigma}_D)$, where $\boldsymbol{\sigma}_D$ represents the configuration within the domain D, and the relevant averages are

$$\langle A\rangle_t = \sum_{\boldsymbol{\sigma}} P(\boldsymbol{\sigma}; t)\, A(\boldsymbol{\sigma}) = \sum_{\boldsymbol{\sigma}_D} Q(\boldsymbol{\sigma}_D; t)\, A(\boldsymbol{\sigma}_D), \tag{3.1}$$

where

$$Q(\boldsymbol{\sigma}_D; t) \equiv \sum_{\boldsymbol{\sigma}\ \boldsymbol{\sigma}_D} P(\boldsymbol{\sigma}; t). \tag{3.2}$$

is the probability distribution for configurations on the domain D. On the other hand, one has from Eq. (2.2) that

$$d\langle A\rangle_t/dt = \sum_{|\mathbf{x}} \sum_{\mathbf{z}|=1} \sum_{\boldsymbol{\sigma}} \delta A(\boldsymbol{\sigma}; \mathbf{x}, \mathbf{z})\, c(\boldsymbol{\sigma}; \mathbf{x}, \mathbf{z})\, P(\boldsymbol{\sigma}; t), \tag{3.3}$$

where $\delta A(\boldsymbol{\sigma}; \mathbf{x}, \mathbf{z}) \equiv A(\boldsymbol{\sigma}^{\mathbf{x},\mathbf{z}}) - A(\boldsymbol{\sigma})$. Let us define the domain interior, I, and surface, S, such that $D = I\cup S$, $I\cap S=\phi$, where $I=\{\mathbf{x}\in D;\ |\mathbf{x}-\mathbf{z}|=1\Rightarrow \mathbf{z}\in D\}$, i.e., I is the set of lattice sites in D having all n.n. as elements of D, while any $\mathbf{x}\in S$ will have a least a n.n. outside D. Thus, Eq. (3.3) may be written as

$$d\langle A(\boldsymbol{\sigma}_D)\rangle_t/dt = \sum_{\substack{|\mathbf{x}-\mathbf{z}|=1\\ \mathbf{x},\mathbf{z}\in I}} \sum_{\boldsymbol{\sigma}_D} \delta A(\boldsymbol{\sigma}_D; \mathbf{x}, \mathbf{z})\, c(\boldsymbol{\sigma}_D; \mathbf{x}, \mathbf{z})\, Q(\boldsymbol{\sigma}_D; t) \tag{3.4}$$

when one assumes that, for any $\mathbf{x}$ and $\mathbf{z}$ belonging to I, every site involved by $c(\boldsymbol{\sigma}; \mathbf{x}, \mathbf{z})$ belongs to D, and that

$$\sum_{\substack{|\mathbf{x}-\mathbf{z}|=1\\ \mathbf{x}\text{ and/or }\mathbf{z}\in S}} \sum_{\boldsymbol{\sigma}} \delta A(\boldsymbol{\sigma}_D; \mathbf{x}, \mathbf{z})\, c(\boldsymbol{\sigma}; \mathbf{x}, \mathbf{z})\, P(\boldsymbol{\sigma}; t) = 0. \tag{3.5}$$

While the former property is fulfilled by every familiar transition probability, e.g., the ones in Refs. [7, 27, 28], the latter is a fundamental approximation in the present method whose influence becomes negligible as D tends to equal the whole lattice Z^d, i.e., varying the size of D leads to a different approximation, as it also occurs in the familiar "cluster variation" method [24] to deal with equilibrium problems.

The simplifying assumption, Eq. (3.5), amounts to neglecting any coupling between the occupation variables in the local domain D and those in the rest of the system, Z^d-D. Further insight into the nature of the approximation, Eq. (3.5), is obtained if we notice that the microscopic dynamical variables in Eq. (3.1) may be written as $A(\boldsymbol{\sigma}_D) = \alpha(\hat{\boldsymbol{\sigma}}_D) + \sigma_{\mathbf{x}}\beta(\boldsymbol{\sigma}_D) + \sigma_{\mathbf{z}}\mu(\boldsymbol{\sigma}_D) + \sigma_{\mathbf{x}}\sigma_{\mathbf{z}}\delta(\boldsymbol{\sigma}_D)$, for all $\mathbf{x}, \mathbf{z}\in D$, where

$\hat{\boldsymbol{\sigma}}_D$ is $\boldsymbol{\sigma}_D$ except for the occupation variables at sites $\mathbf{x}$ and $\mathbf{z}$. Thus, Eq. (3.5) reduces to

$$\sum_{\substack{|\mathbf{x}-\mathbf{z}|=1 \\ \mathbf{x} \text{ and/or } \mathbf{z} \in S}} \langle (\sigma_{\mathbf{z}} - \sigma_{\mathbf{x}})[\beta(\hat{\boldsymbol{\sigma}}_D) - \mu(\hat{\boldsymbol{\sigma}}_D)]\, c(\boldsymbol{\sigma}; \mathbf{x}, \mathbf{z}) \rangle_t = 0 \tag{3.6}$$

implying, for arbitrary β and μ, the cancellation of local currents $j(\sigma; \mathbf{x}, \mathbf{z}) \equiv (\sigma_{\mathbf{z}} - \sigma_{\mathbf{x}})\, c(\boldsymbol{\sigma}; \mathbf{x}, \mathbf{z})$ between points $\mathbf{z}$ and $\mathbf{x}$; in other words, hypothesis (3.5) amounts to neglecting net currents through the surface domain and, consequently, some local fluctuations. This (nonequilibrium) approximation essentially corresponds to the one contained in the Bethe–Peierls theory for equilibrium, i.e, it is a first-order mean field description [30], when D has the minimum allowable size (see below): the consideration of larger domains leads successively to higher order approximations.

The explicit use of the resulting Eq. (3.4) requires further approximations concerning $Q(\boldsymbol{\sigma}_D; t)$. That is, one has exactly that

$$Q(\boldsymbol{\sigma}_D; t) = 1 + \langle \sigma_{\mathbf{x}} \rangle_t \sum_{\mathbf{x} \in D} \sigma_{\mathbf{x}} + \langle \sigma_{\mathbf{x}} \sigma_{\mathbf{y}} \rangle_t \sum_{\mathbf{x}, \mathbf{y} \in D} \sigma_{\mathbf{x}} \sigma_{\mathbf{y}} + \cdots + \Big\langle \prod_{\mathbf{x} \in D} \sigma_{\mathbf{x}} \Big\rangle_t \prod_{\mathbf{x} \in D} \sigma_{\mathbf{x}}, \tag{3.7}$$

where the averages are defined by Eq. (3.5), while one needs to write those coefficients in terms of a few low-order correlation functions. Of course, one should introduce here an approximation which is consistent with the previously selected size of D; e.g., the average $\langle \pi_{\mathbf{x} \in D} \sigma_{\mathbf{x}} \rangle_t$ in Eq. (3.7) may be approximated by a function $\langle \sigma_{\mathbf{x}} \rangle_t$ and $\langle \sigma_{\mathbf{x}} \sigma_{\mathbf{y}} \rangle_t$, where $|\mathbf{x} - \mathbf{y}| = 1$, in order to remain within the above Bethe–Peierls type of description. This means in practice that $Q(\boldsymbol{\sigma}_D; t) \equiv Q(\boldsymbol{\sigma}_D; \langle \sigma \rangle, \langle \sigma\sigma \rangle_{nn}; t)$ can be written as a function of (only) the densities of n.n. pairs $++$, $+-$, and $--$ (where $+$ represents a site occupied by a particle, and $-$ represents a hole) which will be represented by u, s, and z, respectively, with $u + s + z = 1$. As we shall see, such an approximation, which is consistent with the choice of the minimum allowable size for D (to be defined precisely in the next section) already provides an interesting description for the model presented in Section 2.

4. Explicit Time-Evolution Equations: Pair Approximation

The minimum domain D which allows a kinetic first-order mean-field approximation is

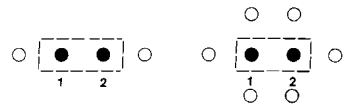

for one- and two-dimensional systems, respectively; the circles denote lattice sites (which may be occupied or vacant) and the discontinuous line encloses the only n.n. pair belonging to I (the interior n.n. sites being labelled 1 and 2, respectively). In general, the minimum domain for a d-dimensional system may be characterized by the occupation variables at the (two) sites in I, say σ_1 and σ_2, and by the number of particles in D_1 and D_2, say N_1^+ and N_2^+, where $D_1 \cap D_2 = \phi$, $D_1 \cup D_2 = S$, and D_i contains $2d$-1 sites around the interior site i. Thus, the associated probabilities for the occurrence of a given domain configuration are, within the approximation of interest

$$Q_{\sigma_1, \sigma_2, N_1^+, N_2^+}(u; n) = g(N_1^+)\, g(N_2^+)\, p(\sigma_1, \sigma_2)\, p(+|\sigma_1)^{N_1^+} \times p(-|\sigma_1)^{2d-1-N_1^-}\, p(+|\sigma_2)^{N_2^+}\, p(-|\sigma_2)^{2d-1-N_2^-}, \tag{4.1}$$

where

$$g(N_i^+) = \begin{bmatrix} 2d-1 \\ N_i^+ \end{bmatrix} \tag{4.2}$$

is the degeneracy associated with D_i, $i = 1, 2$, $p(\sigma, \sigma')$ represents the joint probability for the n.n. pair of occupation variables (σ, σ'), and $p(\sigma|\sigma') = p(\sigma, \sigma')/p(\sigma')$ is a conditional probability with $p(\sigma)$ the probability of σ; one has, according to the definitions at the end of Section 3, that $p(+,+) = u$, $p(-,-) = z$, $p(+,-) = p(-,+) = 1 - u - z$, and $p(+,+) + p(+,-) = p(+) = n$, the particle density, while $p(-,-) + p(-,+) = p(-) = 1 - n$, $z = 1 - 2n + u$, and $p(+,-) = n - u$ so that the pair probabilities are determined once n and u are specified.

The system dynamics described in Section 2 consists of interchanges of the occupation variables at a n.n. pair of sites, so that $n = \text{const.}$ during the system time evolution. Moreover, the first sum in Eq. (3.4) restricts the moves to the pairs in I, i.e., to sites 1 and 2 for the above choice of D. Consequently, the macroscopic variable of interest is the density of n.n. pairs of particles, u, which is a measure of the system energy whose evolution follows from Eqs. (3.4) and (4.1) as

$$du/dt = 2 \sum_{N_1^+ = 0}^{2d-1} \sum_{N_2^+ = 0}^{2d-1} (N_2^+ - N_1^+)\, \Phi[\delta H(N_1^+, N_2^+; +, -)] \times Q_{\ldots, N_1^+, N_2^+}(u). \tag{4.3}$$

The present method is readily generalized to include other dynamical processes e.g., the case of spin-flip dynamics where one would obtain from (3.4), in addition to (4.3), a similar equation for n or z, and it allows the consideration of rather general choices for the transition probabilities c. We shall consider in the following the case of a particle conserving dynamics with a transition probability dependent upon a parameters such as temperature T, particle density n, external electric field E, etc., and on the change in the system configurational energy (2.1), i.e., $\delta H(N_1^+, N_2^+; \sigma_1, \sigma_2) = -4J(N_1^+ - N_2^-)(\sigma_2 - \sigma_1)$, produced by the allowed interchanges involving sites 1 and 2.

Summing up, the evolution with time of macroscopic quantities follows from Eqs. (4.3), (4.1), and (3.4). A necessary condition for the stability of the corresponding stationary solution, $F(u_{st}) = 0$, is that

$$(\delta F/\delta u)_{u=u_{st}} < 0, \tag{4.4}$$

where $F(u, t)$ represents the r.h.s. of Eq. (4.3). The critical condition $(\delta F/\delta u)_{st} = 0$ may then correspond to a phase transition. The study in Refs. [8, 11] performs an interpretation of stability which is essentially similar to ours here. Section 10 considers further questions related to the stability of a particular steady state.

5. One-Dimensional System

The fact that many solid electrolytes apparently suffer low dimensionality effects [20, 22] grants an unusual practical interest to DDS when $d \leqslant 2$. We apply here the method developed in Sections 3 and 4 to the case $d = 1$, i.e., when the lattice forms a large closed line under the presence of a uniform electric field $\mathbf{E} = E\hat{\mathbf{x}}$, where $E > 0$ and $\hat{\mathbf{x}}$ defines a positive direction along the line. The dynamics then proceeds according to a transition probability per unit time given by

$$w(\delta H) = \tfrac{1}{2}[\Phi_+ + \Phi_-], \tag{5.1}$$

where $\Phi_\pm$ corrspond respectively to the hopping processes along the $\pm\hat{\mathbf{x}}$ directions, and we shall consider explicitly the choices (2.4) and (2.5); that is, either

$$\Phi_\pm = \min[1, \exp(\beta\{-\delta H \pm E\})] \qquad \text{(Metropolis)} \tag{5.2}$$

or else

$$\Phi_\pm = \{1 + \exp[-\beta(-\delta H \pm E)]\}^{-1} \qquad \text{(Kawasaki);} \tag{5.3}$$

we shall write $\beta E \equiv E$ for simplicity in the following. This amounts to considering separately, with equal a priori probabilities, the possibility of jumps in directions $\pm\hat{\mathbf{x}}$ biased with a probability which favors the jumps along the field direction and depends on the change in the system energy produced by the attempted jump. When $E = 0$, the processes based on (5.2) and (5.3) reduce respectively to the ones discussed by Metropolis *et al.* [27] and by Kawasaki [28], both leading to the same Gibbs state at temperature β, while (5.2) and (5.3) may produce different (nonequilibrium) steady states when $E > 0$.

Time Evolution

The resulting time evolution when $d = 1$ follows from Eqs. (4.1)–(4.3) as

$$du/dt = F(u; n, \beta, E, J) \tag{5.4a}$$

with

$$F = \frac{2(n-u)}{n(1-n)}[(n-u)^2 w(-4J) - u(1-2n+u)\, w(4J)], \tag{5.4b}$$

where u represents the density of $++$ n.n. pairs, n is the particle density, $J > 0$ (< 0) for "ferromagnetic" ("antiferromagnetic") interactions, and one has

$$w(4|J|) = \begin{cases} \tfrac{1}{2}[1 + \exp(-4\beta|J| - E)] & E \geqslant 4\beta|J| \\ \exp(-4\beta|J|)\cosh E, & E \leqslant 4\beta J \end{cases} \tag{5.5a}$$

and

$$w(-4|J|) = \begin{cases} \tfrac{1}{2}[1 + \exp(4\beta|J| - E)], & E \geqslant 4\beta|J| \\ 1, & E \leqslant 4\beta J \end{cases} \tag{5.5b}$$

for the choice (5.2), and

$$w(\pm 4|J|) = \tfrac{1}{2}\{[1 + \exp(\pm 4\beta|J| - E)]^{-1} + [1 + \exp(\pm 4\beta|J| + E)]^{-1}\} \tag{5.6}$$

for the choice (5.3).

The general solution of Eq. (5.4) is

$$\frac{[2\delta(n-u) + w(4J) - \alpha]^{\alpha}}{[2\delta(n-u) + w(4J) + \alpha]^{\alpha}}[2n(1-n)(n-u)^2\delta]^{-1} = \exp(-4t + C_0), \tag{5.7a}$$

where $\delta \equiv w(-4J) - w(4J)$,

$$\alpha \equiv [w(4J)^2 + 4n(1-n)\,\delta w(4J)]^{1/2}, \tag{5.7b}$$

$\alpha^\pm \equiv w(4J)/\alpha \pm 1$, and C_0 is a constant related to the initial conditions; one also has the special solutions

$$u = n - (n - u_0)(at + 1)^{-1/2}, \tag{5.8a}$$

where $u_0 = u(t = 0)$ and

$$a = 4(n - u_0)^2[n(1-n)]^{-1} w(-4J), \tag{5.8b}$$

when $w(4J) = 0$ and $w(-4J) > 0$,

$$u \approx [4w(4J)\, t]^{-1} \tag{5.9}$$

when $w(4J) > 0$, $w(-4J) = 0$, and $n = 1/2$ ($n > 1/2$ produces a more involved expression), and

$$u = n - n(1-n)\{1 - [(n^2 - u_0)/(n - u_0)]\exp[-2w(4J)\, t]\}^{-1} \tag{5.10}$$

when $w(4J) = w(-4J) > 0$. Thus, the system may show up an exponential decay as in (5.10), or a much slower relaxation as in (5.8) and (5.9); the latter corresponds to the presence of a critical point at $\beta = \infty$.

Steady States

The general solution (5.7) may be seen to lead as $t \to \infty$ to the stationary solution

$$u_{st} = n - \tfrac{1}{2}[-w(4J) \pm \alpha]\,\delta^{-1}, \tag{5.11}$$

while the special solutions (5.8), (5.9), and (5.10) produce respectively the steady states:

$$u_{st} = n, \qquad \text{as} \quad \beta \to \infty \quad \text{when} \quad J > 0 \tag{5.12}$$

for all finite E,

$$u_{st} = 0,\ 2n-1, \qquad \text{as} \quad \beta \to \infty \quad \text{when} \quad J < 0 \tag{5.13}$$

for all finite E and $n \geqslant \tfrac{1}{2}$, and

$$u_{st} = n^2, \qquad \text{for all } J, \tag{5.14}$$

either as $\beta \to 0$ for all finite E or as $E \to \infty$ for all β. One may notice here, in particular, that both dynamics, (5.2) or (5.3), tend to destroy correlations when $\beta \to 0$ or else when $E \to \infty$ and that the state for $\beta \to \infty$, $E > 0$, is practically indistinguishable from the corresponding equilibrium state ($E = 0$) when $J > 0$ and when $J < 0$ with $n = \tfrac{1}{2}$ (the behavior strongly depends on n otherwise).

The stability of the above solutions is related to the sign of $(\delta F/\delta u)_{st}$; i.e., stability requires that

$$3\delta(n-u)^2 + w(4J)[n(1+n) - 2u] > 0. \tag{5.15}$$

It thus follows that only the negative sign in Eq. (5.11) produces a stable solution and, concerning the special solutions: (5.14) is always stable, (5.12) has a critical stability; i.e., the expression in (5.15) equals zero when $u = n$ and $w(4J) = 0$, and the two solutions (5.13) are only stable for certain values of n. i.e. $u_{st} = 0$ is stable for $n < \tfrac{1}{2}$ and has a neutral stability when $n = \tfrac{1}{2}$, while $u_{st} = 2n - 1$ is stable for $n > \tfrac{1}{2}$.

Current and Conductivity

The external electric field $E\hat{\mathbf{x}}$ acting on the ions induces a net current along the $\hat{\mathbf{x}}$ direction which may be defined as:

$$j(t; \beta, E, n) = \lim_{\delta t \to 0} (N\,\delta t)^{-1}\,[N_{\hat{\mathbf{x}}}(t, \delta t) - N_{-\hat{\mathbf{x}}}(t, \delta t)]; \tag{5.16a}$$

N represents the number of particles in the system, and $N_{\pm\hat{\mathbf{x}}}(t, \delta t)$ is the number of particles hopping to their n.n. empty positions in the $\pm\hat{\mathbf{x}}$ direction between times t and $t + \delta t$. According to Section 4, the current may also be written as

$$j(t; \beta, E, n) = \sum_{\substack{N_1^+ = 0,1 \\ N_2^+ = 0,1}} \{\Phi_+[-4J(N_1^+ - N_2^+)] - \Phi_-[-4J(N_1^+ - N_2^+)]\}\, Q_{+,-,N_1^+,N_2^+}, \tag{5.16b}$$

where $\Phi_\pm$ are defined by either (5.2) or (5.3).

The explicit computation of (5.16) produces different qualitative behaviors as one varies the dynamics, field strength, and kind of interactions; namely, one has for the choice (5.2) that

$$j(t; \beta, E, n) = \frac{n-u}{n(1-n)}\,[(n-u)(1-2n+2u)(1-e^{-E}) + u(1-2n+u)(1-e^{-E-4\beta J}) + (n-u)^2(1-e^{-E+4\beta J}), \qquad E \geqslant 4\beta|J|, \tag{5.17}$$

$$j(t; \beta, E, n) = \frac{n-u}{n(1-n)}\,[(n-u)(1-2n+2u)(1-e^{-E}) + 2u(1-2n+u)\,e^{-4\beta J}\sinh(E), \qquad E \leqslant 4\beta J,\ J > 0 \tag{5.18}$$

$$j(t; \beta, E, n) = \frac{n-u}{n(1-n)}\,[(n-u)(1-2n+2u)(1-e^{-E}) + 2(n-u)^2\,e^{-4\beta|J|}\sinh(E), \qquad E \leqslant 4\beta|J|,\ J < 0, \tag{5.19}$$

while it follows for the choice (5.3) that

$$j(t; \beta, E, n) = \frac{2(n-u)}{n(1-n)}\sinh(E)\left\{\frac{(n-u)(1-2n+2u)}{2(1+\cosh(E))} + [u(1-2n+u) + (n-u)^2][(e^{-4\beta|J|} + e^{-E})(1+e^{4\beta J+E})]^{-1}\right\} \tag{5.20}$$

for all J and E, where $u = u(t)$. The infinite field limit for both dynamics is $j(t; \beta, \infty, n) = n - u(t)$; i.e., it is simply related to the behavior of the energy. Several other limiting conditions may be worked out from the above expressions as well; it follows in particular that limits concerning β and E, for instance, do not commute in general. On the other hand, the stationary values of the current, j_{st}, easily follow by combining Eqs. (5.17)–(5.20), or the corresponding ones for different limiting conditions, with Eqs. (5.11)–(5.14) for u_{st}.

Figures 1 and 2 illustrate the behavior of j_{st} with T, E, and sign of J. Figure 1

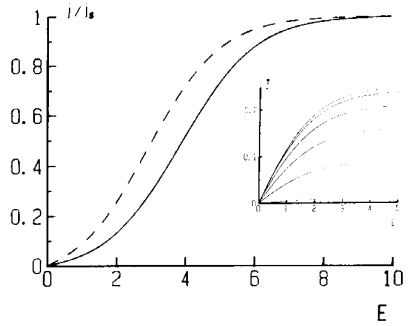

FIG. 1. The stationary current (normalized to the saturation, infinite-field, value) versus field strength for the one-dimensional DDS in Section 5 when $J>0$ (ferromagnetic case), $T=1$ ($J/k\equiv 1$), and for the Kawasaki type of dynamics (5.3). The solid line is for $n=\frac{1}{2}$, and the dashed one is for $n=0.1$. The inset represents j_{st} when $\beta\to 0$ for different densities: $n=0.5$, 0.4, 0.3, 0.2, and 0.1 from top to bottom.

represents $j_{st}(E)$ for the ferromagnetic ($J>0$) case; the antiferromagnetic case is qualitatively similar, except that j_{st} saturates around $E=5$ and the increase for small fields is more abrupt, especially for small n where d^2j_{st}/dE^2 is negative (unlike the case in Fig. 1). The use of a different dynamics produces no qualitative change, except that (5.2) induces a discontinuity of dj_{st}/dE at $E=4\beta J$; this is, however, just

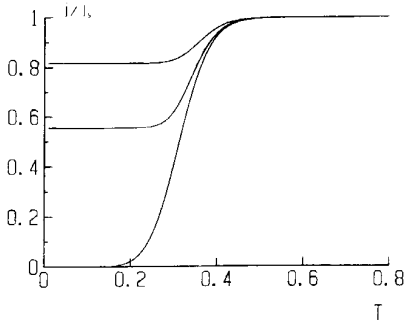

FIG. 2. The stationary current, as in Fig. 1, versus temperature when $E=10$ and $J<0$ (antiferromagnetic case) for different densities: $n=0.3$, 0.4, and 0.5 from top to bottom. The ferromagnetic case has a behavior qualitatively similar to the one shown by the graph $n=\frac{1}{2}$ here.

an artifact of the Metropolis transition probability. Figure 2 represents $j_{st}(T)$ for the antiferromagnetic case; the ferromagnetic case has, independently of the values of n, a behavior qualitatively similar to the one shown by the graph for $n=\frac{1}{2}$ in Fig. 2. That is, the present one-dimensional systems belong to two different well-defined classes. The first one includes the cases $J<0$ with $n\neq\frac{1}{2}$; this is characterized (as it is illustrated for $E=10$ by the two graphs near the top in Fig. 2) by qualitatively similar, good conductor, states at low and high temperatures, with however a sudden increase around $T=4/E$. The second class includes the cases $J<0$ with $n=\frac{1}{2}$ (the one which is illustrated by the bottom graph in Fig. 4) and $J>0$ with any density; this shows a continuous changeover from an insulator state wehn $T\ll 4/E$ to a good conductor state when $T>4/E$. The qualitative differences between those two classes are clearly a consequence of the degeneracy of the ground antiferromagnetic states when $n<\frac{1}{2}$, a fact which favors large stationary currents at low temperatures; those qualitative differences in the model may be relevant to understanding the behavior shown by real super ionic conductors with low dimensionality effects [19, 20, 22].

The stationary current for small fields may be written, by developing the above expressions for $t\to\infty$ around $E=0$, as

$$j_{st}(\beta, E, n)=\frac{n-u_{st}^0}{n(1-n)}\left[(n-u_{st}^0)(u_{st}^0+z_{st}^0)+\phi_{st}^0\right]E+O(E^2) \tag{5.21}$$

where $u_{st}^0\equiv u_{st}(E=0)$, $z_{st}^0\equiv z_{st}(E=0)$, $z=1-2n+u$, and

$$\phi_{st}^0\equiv -2u_{st}^0 z_{st}^0\exp(-4\beta J) \tag{5.22}$$

for $J>0$,

$$\phi_{st}^0\equiv 2(n-u_{st}^0)^2\exp(-4\beta|J|) \tag{5.23}$$

for $J<0$, both for the Metropolis type dynamics (5.2), and

$$\phi_{st}^0\equiv 2[u_{st}^0 z_{st}^0+(n-u_{st}^0)^2]\,e^{4\beta|J|}(1+e^{4\beta|J|})^{-2}-(n-u_{st}^0)(u_{st}^0+z_{st}^0)/2 \tag{5.24}$$

for the Kawasaki-type dynamics (5.3).

The electric conductivity then follows as

$$s=(dj_{st}/dE)_{E=0}; \tag{5.25}$$

this leads when $n=\frac{1}{2}$ to the expressions as a function of temperature,

$$s=e^{-2\beta|J|}\left[1+e^{-2\beta|J|}\right]^{-2},\qquad J<0,\ n=\tfrac{1}{2} \tag{5.26}$$

for the Metropolis case, and

$$s=e^{-2\beta|J|}\left[2(1+e^{-4\beta|J|})(1+e^{-2\beta|J|})\right]^{-1},\qquad J<0,\ n=\tfrac{1}{2} \tag{5.27}$$

for the Kawasaki case, both when the interactions are antiferromagnetic, while this is related to te electric conductivity of the corresponding ferromagnetic system by

$$s(J>0) = \exp[-2\beta |J|]\, s(J<0) \tag{5.28}$$

for both dynamics.

The first consequence here is that the electric conductivity of a ferromagnetic system at given temperature is always smaller than that of the antiferromagnetic counterpart at the same temperature; i.e., repulsive interactions favor the system conductivity more than attractive interactions do. Figure 3 represents the behavior implied by Eqs. (5.26)–(5.28). An interesting result in Fig. 3 concerns the influence of different dynamics on the properties of the (nonequilibrium) steady state. That is, while the maxima of s always occur at high temperatures, where the thermal motion favors the drift of the field, and $s(K) \to 0$ as $|K| \equiv |J|/kT \to \infty$, when the system tends to be more ordered, there is a maximum of $s(K)$ for $K \leqslant 0$ *only* when the dynamical microscopic process is of the Kawasaki type. This seems related to the fact, which is familiar from Monte Carlo simulations, that Kawasaki dynamics has lower efficiency (in the sense that it allows more transitions per unit time which increases the system energy and, consequently, larger fluctuations) than the

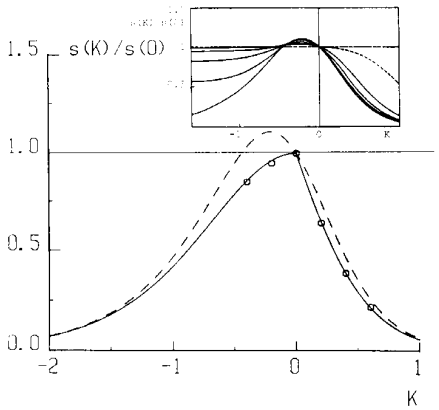

FIG. 3. The electric conductivity at zero field. Eqs. (5.25)–(5.28), normalized to the infinite temperature value, as a function of $K = J/kT$ for Metropolis-type (solid line) and Kawasaki-type (dashed line) dynamics when $n = \frac{1}{2}$. The circles represent MC data for a one-dimensional DDS with Metropolis dynamics [2]. The inset represents exact results for different values of n (as shown) in a related model [31].

Metropolis one; the extra fluctuations favor the appearance of a maximum conductivity state in the case of the antiferromagnetic system before one reaches the infinite temperature limit.

Figure 3 compares our results for a Metropolis dynamics with some available Monte Carlo data which refer essentially to the same model [2]; the agreement is excellent; in particular, both reveal a discontinuity of $ds(K)/dK$ at $K = 0$ which is another distinguishing feature of Metropolis dynamics. Also interesting is the comparison with a model by Dieterich *et al.* [31], where a certain transition probability differing from the ones considered here allows an exact evaluation of $s(K)$. As depicted by the inset in Fig. 3, this has a behavior qualitatively similar to the one shown by our system with Kawasaki dynamics, and it satisfies

$$s(K \to -\infty)/s(K \to 0) = (2n-1)/n^2 \tag{5.29}$$

which is also a characteristic or our system with both Metropolis and Kawasaki dynamics. There are a number of other related models [19, 31–36], usually developed to study specific questions, whose behavior may generally be understood at the light of the present analysis; cf. Ref. [19], for instance.

Specific Heat and Fluctuations

The system configurational energy per lattice sites implied by the Hamiltonian (2.1) is $<e> = \langle H/N \rangle = -4Ju$. In the stationary regime, one may define a (nonequilibrium) "specific heat" as

$$C \equiv d\langle e \rangle_{st}/dT = -(4J/T^2)\, du_{st}/d\beta \tag{5.30}$$

whose behavior is illustrated by Fig. 4 in the case of ferromagnetic interactions and Kawasaki dynamics (a different choice for dynamics and/or interactions produces the same qualitative behavior). This reveals that the maximum which characterizes the equilibrium ($E = 0$) one-dimensional states increases and shifts toward smaller temperatures as E is increased, that the location of the maximum is at $\beta_m \approx E/4$ for large enough fields (i.e., around the mean temperature locating the transition form insulator to good conductor states we described before), and that C tends to a Dirac delta function at $T = 0$ as $E \to \infty$.

An interesting question here concerns the existence of a fluctuation-dissipation theorem, i.e., the relation between the quantity (5.30) and the energy mean-squared fluctuations $\delta^2 e \equiv \langle e^2 \rangle - \langle e \rangle^2$ where the average is to be interpreted as in Eq. (3.1) with a probability $Q(\boldsymbol{\sigma}_D)$ given by Eq. (4.1). It thus follows that $\langle e \rangle = -4Ju$, in accordance with (2.1), and that

$$\delta^2 e = (4J/3n)^2\, u(2u^2 + 4un - 9un^2 + 3n^2). \tag{5.31}$$

When one uses here (and in Eq. (5.30)) the general solution (5.11), it follows a relation of the form

$$\delta^2 e = f(n, T; w)\, C; \tag{5.32}$$

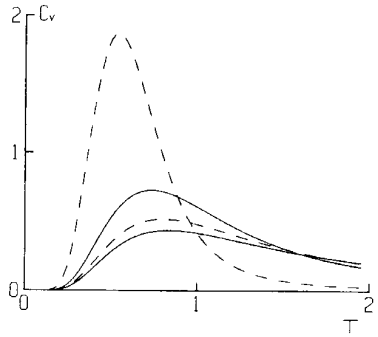

FIG. 4. Temperature dependence of the (nonequilibrium) "specific heat," as defined by Eq. (5.31), for the one-dimensional DDS with ferromagnetic interactions and Kawasaki-type dynamics for different values of the fields: $E=0$, 1, 2, and 5 correspond respectively to the different curves with increasing maximum.

that is, the ratio between $\delta^2 e$ and C involves a functional dependence on w in general. By introducing detailed balance, $w(4J)=\exp(-4J)\,w(-4J)$, into the expression (5.32), f becomes, however, independent of w, and one also has, as expected, that $f(n=1/2,\ T)=kT^2$.

Correlations

The kinetic cluster-variation method also allows the computation of correlation functions, e.g.,

$$\langle \sigma_{j_1}\cdots\sigma_{j_k}\rangle=\sum_{\boldsymbol{\sigma}}\sigma_{j_1}\cdots\sigma_{j_k}P(\boldsymbol{\sigma}), \tag{5.33}$$

$\langle \sigma_{j_1}(t)\,\sigma_{j_2}(t+t')\rangle$, etc. Here $j_1, j_2, \ldots, j_k$ represent any set of k sites in the lattice, and we shall assume they are ordered, $j_1<j_2<\cdots<j_k$, along the line. We may write the philosophy of that method that

$$P(\boldsymbol{\sigma})=cp(\sigma_1)\prod_{j=1}^{N-1}\langle\sigma_j|\bar{p}|\sigma_{j+1}\rangle, \tag{5.34}$$

where it follows that $c=1$ as a consequence of the normalization $\sum_{\sigma}P(\boldsymbol{\sigma})=1$, and the "transfer matrix" [37] is

$$\bar{p}=\begin{bmatrix} \dfrac{u}{n} & \dfrac{n-u}{n} \\[2ex] \dfrac{n-u}{1-n} & \dfrac{1-2n+u}{1-n} \end{bmatrix} \tag{5.35}$$

with eigenvalues 1 and $\Omega\equiv(u-n^2)/n(1-n)<1$. The spatial correlation function follows then as

$$\langle \sigma_{j_1}\cdots\sigma_{j_k}\rangle=n\prod_{r=1}^{k-1}[n+(1-n)\,\Omega^{j_{r+1}-j_r}]. \tag{5.36}$$

That is, $\langle\sigma_0\rangle=n$ and

$$G(j)\equiv\langle\sigma_0\sigma_j\rangle-n^2=n(1-n)[(u-n^2)/(n(1-n))]^j, \qquad j>0 \tag{5.37}$$

and the structure function, defined here as

$$S(k)=\sum_{r=-N/2}^{N/2}e^{ikra}G(ra) \tag{5.38}$$

is given by

$$S(k)=n(1-n)\frac{1-\Omega^2}{1+\Omega^2-2\Omega\cos(k)} \tag{5.39}$$

for the infinite, $N\to\infty$, system and $a=1$. The long range order limit, $S(k=0)$ for $J>0$ and $S(k=\pi)$ for $J<0$, diverges as $\Omega\to\pm1$ respectively; i.e., there is a critical point at $T=0$ for the ferromagnetic system, where $u=n$, and also for the antiferromagnetic system when $n=\frac{1}{2}$; otherwise ($n=\frac{1}{2}$ and $J<0$) the degeneracy of the ground state precludes long range order at any temperature, excluding the trivial cases $n=1, 0$.

6. THE PROBLEM IN TWO DIMENSIONS

An outstanding feature of the model of interest in two (or more) dimensions is the essential anisotropy of the involved transition probabilities; these may be written in general as

$$c_E(\boldsymbol{\sigma};\mathbf{x},\mathbf{y})=\begin{cases} c_{\hat{\mathbf{e}}}(\boldsymbol{\sigma};\mathbf{x},\mathbf{y}), & \text{when} \quad \mathbf{x}-\mathbf{y}=\pm\hat{\mathbf{e}} \\ c_{\hat{\mathbf{e}}_\perp}(\boldsymbol{\sigma};\mathbf{x},\mathbf{y}), & \text{when} \quad \mathbf{x}-\mathbf{y}=\pm\hat{\mathbf{e}}_\perp \\ 0, & \text{otherwise} \end{cases} \tag{6.1}$$

where $\hat{\mathbf{e}}$ and $\hat{\mathbf{e}}_\perp$ are unitary vectors defining respectively the "vertical" and "horizontal" principal directions of the lattice, $\mathbf{E}=E\hat{\mathbf{e}}$, and $c_{\hat{\mathbf{e}}}$ and $c_{\hat{\mathbf{e}}_\perp}$ are defined in accordance with (2.3), allowing, however, for different functions Φ, say Φ_{v} and Φ_{h}, for vertical and horizontal transitions. As a consequence, the resulting master equation (2.2) contains two classes of terms associated respectively with transitions along $\hat{\mathbf{e}}$ and $\hat{\mathbf{e}}_\perp$; we shall denote by $\Gamma_\parallel$ and by $\Gamma_\perp$ the a priori frequencies for the respective transitions and define $\Gamma\equiv\Gamma_\parallel/\Gamma_\perp$.

A series of Monte Carlo studies [2–6] have revealed that, in the two-dimensional case with attractive interactions ($J>0$): (a) there is a (nonequilibrium) second-order phase transition at $T_c(E)$ when $n\approx\frac{1}{2}$, with $T_c(E)$ increasing with E (on the contrary, $T_c(E)$ happens to decrease with increasing E when $J<0$); (b) the phase transition becomes discontinuous for $n\ll\frac{1}{2}$; (c) the low-temperature, ordered phase is always highly anisotropic, with strip-like configurations, as in Fig. 5, parallel to the field direction; (d) the particle current $j_{st}(T)$ has a discontinuous slope at the transition temperature; and (e) the system has *some* mean-field features, at least in certain limiting conditions, but it cannot be described by a classical, mean-field theory for all values of Γ and E, e.g., its critical exponents for $\Gamma=1$ and $E\to\infty$ seem to differ from both the equilibrium Onsager values and the classical Landau ones.

The same problem has been studied before by applying renormalization group techniques to simplified continuum models [9–10], by means of exact computations in small lattices [29]. More pertinent to the present study is the work of van Beijeren and Schulman [7], who found an exact expression for the stationary probability $P_E(\boldsymbol{\sigma})$ in the limit $\Gamma\to\infty$, $E\to\infty$ when the function Φ in Eq. (2.3) has the form (2.6); that limit was considered also by Krugg *et al.* [8] by using different techniques to confirm and extend the results in Ref. [7].

The rest of this paper is devoted to finding an analytical solution of the two-dimensional model system which generalizes the conditions considered before. We first generalize the model by van Beijeren and Schulman to include, still within the limit $\Gamma\to\infty$, arbitrary transition probabilities and finite values of E; our equations

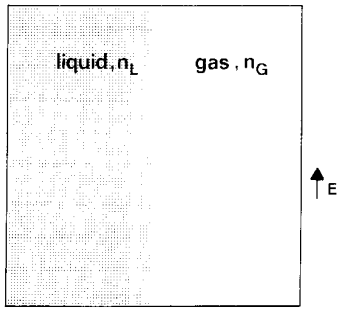

FIG. 5. A typical configuration of the two-dimensional DDS with ferromagnetic interactions below the transition temperature, as obtained in a MC experiment [5] on a 100×100 lattice with $n=\frac{1}{2}$ under an infinite field at $T=0.80T_c(0)$, the corresponding equilibrium critical temperature. The situation is similar for all $T<T_c(E)$, the nonequilibrium critical temperature, with coexisting phases of densities $n_L(T)$ and $n_G(T)$, respectively, while the system is macroscopically homogeneous for all $T>T_c(E)>T_c(0)$.

are also more general in the sense that, unlike previous formalisms, they allow the consideration of the case $\Gamma\to0$. The solution of the model, which reproduces the known results as $E\to\infty$, is based on the results in Sections 3–5 and it uses, to some extent, techniques similar to those of Krug *et al.* We then turn, in Section 9, to a more general point of view which allows the consideration of arbitrary values for Γ and E; this solution is based on the kinetic cluster-variation method and on the phenomenological observation (c) noted above. The resulting description has a well-defined mean-field nature, so that its comparison with the available Monte Carlo data may in principle somewhat clarify the situation concerning point (e).

7. The Fast Rate Limit for Arbitrary Fields

In the limit $\Gamma\to\infty$, the transitions along the field direction are so frequent, as compared to those perpendicular to **E**, that one may consider the system as a collection of (vertical) columns which immediately stabilize; i.e., they reach the new steady state with the current number of particles after each (horizontal) transition between neighboring columns [7]. This implies in particular that one may distinguish two-different well-defined times scales: On a *microscopic* time scale, the stationary condition $dP_E(\boldsymbol{\sigma};t)/dt=0$ holds and $c_{\hat{\mathbf{e}}_\perp}(\boldsymbol{\sigma};\mathbf{x},\mathbf{y})=0$; i.e., only transitions within each column can occur. It then follows that

$$P_E(\boldsymbol{\sigma})=\prod_i \pi_E(\boldsymbol{\sigma}_i;\eta_i;\boldsymbol{\eta}) \tag{7.1}$$

where $\pi_E(\boldsymbol{\sigma}_i;\eta_i;\boldsymbol{\eta})$ represents the probability that the ith column with η_i particles has the configuration $\boldsymbol{\sigma}_i$, and $\boldsymbol{\eta}$, $(\boldsymbol{\eta}_i)\equiv\eta_i$, indicates that π_E may depend on the occupation of the surrounding columns. It also follows that

$$\sum_{\mathbf{x}-\mathbf{y}=\pm\hat{\mathbf{e}}} [c_{\hat{\mathbf{e}}}(\boldsymbol{\sigma}^{x,y};\mathbf{x},\mathbf{y})\,\pi_E(\boldsymbol{\sigma}_i^{x,y};\eta_i;\boldsymbol{\eta})-c_{\hat{\mathbf{e}}}(\boldsymbol{\sigma};\mathbf{x},\mathbf{y})\,\pi_E(\boldsymbol{\sigma}_i;\eta_i;\boldsymbol{\eta})]=0, \tag{7.2}$$

where $\mathbf{x}$ belongs to the ith column. One has a *macroscopic* time scale, however, that

$$P_E(\sigma;t)=p_E(\boldsymbol{\eta};t)\prod_i \pi_E(\boldsymbol{\sigma}_i;\eta_i;\boldsymbol{\eta}), \tag{7.3}$$

where $p_E(\boldsymbol{\eta};t)$ represents the probability that the columns have η_i, $i=1,2,\ldots,M$, particles at time t. The latter satisfies the master equation:

$$\frac{dp_E(\boldsymbol{\eta};t)}{dt}=\sum[c(\boldsymbol{\eta}',\boldsymbol{\eta})\,p_E(\boldsymbol{\eta}';t)-c(\boldsymbol{\eta},\boldsymbol{\eta}')\,p_E(\boldsymbol{\eta};t)] \tag{7.4}$$

with

$$c(\boldsymbol{\eta}',\boldsymbol{\eta})\equiv N\langle\Phi_h[\beta H(\boldsymbol{\sigma}^{x,y})-\beta H(\sigma)]\rangle, \qquad \mathbf{x},\mathbf{y}=\pm\hat{\mathbf{e}}_\perp, \tag{7.5}$$

where N is the number of lattice sites in each column and $\langle \cdot \rangle_{\eta}$ represents an ensemble average with the probability (7.1); $\sum_{\eta} p_E(\eta; t) = 1$.

Consequently, the original two-dimensional problem transforms in the limit $\Gamma \to \infty$ into two one-dimensional problems which are governed respectively by Eqs. (7.2) and (7.4). This fact was noted before by van Beijeren and Schulman [7]; previous work [7, 8], however, also considers the situation in which any transition opposite to **E** is forbidden and those in the direction of **E** are always allowed unless they violate the hard-core exclusion. That strong field limit washes out all correlations within each column and solves the problem of computing explicitly $\langle \cdot \rangle_{\eta}$ which then simply corresponds to a random distribution of the particles in each column. Instead, we shall compute here $c(\eta', \eta)$, as given by Eq. (7.5), for arbitrary values of E. This will require the following steps: (i) solve Eq. (7.2) by using the kinetic cluster variation method. This means in practice to obtain the values for $\mathbf{u}$, the density of $++$ pairs in each column, $(\mathbf{u})_i \equiv u_i = u_i(\mathbf{n})$, $i = 1, 2, ..., M$, where $n_i = \eta_i / N$ is the density of particles at column i, $(\mathbf{n})_i \equiv n_i$. (ii) Find an explicit expression for (7.5) by using the philosophy of the method in Sections 3–5 and the solution $u_i = u_i(\mathbf{n})$ from the previous step. (iii) Solve Eq. (7.4) for large N by using the Ω-expansion technique [38]. As in the work by Krug *et al.* [8].

Step (i). Let us consider three neighboring columns, labelled $i = 1, 2, 3$, characterized respectively by densities n_i and by the unknowns u_i. The probability of a local configuration such that

$$\begin{array}{ll} \text{column } i = & \begin{array}{ccc} 1 & 2 & 3 \end{array} \\ \text{occupation variables} & \begin{cases} & \sigma_4 & \\ \sigma_2 & 0 & \sigma_6 \\ \sigma_1 & 1 & \sigma_5 \\ & \sigma_3 & \end{cases} \end{array}$$

is given by

$$Q_{1,0}(\sigma_1, ..., \sigma_6) = (n_2 - u_2) \frac{u_2^{\sigma_3}}{n_2} (n_2 - u_2)^{1 - \sigma_3} \times \frac{z_2^{1 - \sigma_4}}{1 - n_2} (n_2 - u_2)^{\sigma_4} q_1(\sigma_1, \sigma_2)\, q_3(\sigma_5, \sigma_6), \tag{7.6}$$

where

$$q_i(\sigma, \sigma') = \begin{cases} u_i, & \text{if } \sigma = \sigma' = 1 \\ n_i - u_i, & \text{if } \sigma = 1, \sigma' = 0 \\ & \text{or } \sigma = 0, \sigma' = 1 \\ z_i, & \text{if } \sigma = \sigma' = 0, \end{cases} \tag{7.7}$$

$z_i = 1 - 2n_i + u_i$. Thus, Eq. (4.3) reads

$$\frac{du_2}{dt} = \sum_{\sigma_1, ..., \sigma_6} (\sigma_4 - \sigma_3)\, \Phi_t(\delta H)\, Q_{1,0}(\sigma_1, ..., \sigma_6); \tag{7.8}$$

$\delta H = -4J(\sigma_2 + \sigma_4 + \sigma_6 - \sigma_1 - \sigma_3 - \sigma_5)$, and Φ_t is the transition probability acting within each column. The corresponding stationary solution is

$$\begin{aligned} &[\Theta_2(0) + \Theta_2(8J)][(n_1 - u_1)(u_3 + z_3) + (n_3 - u_3)(u_1 + z_1)] \\ &\quad + \Theta_2(4J)[2(n_1 - u_1)(n_3 - u_3) + (u_1 + z_1)(u_3 + z_3)] \\ &\quad + [\Theta_2(-4J) + \Theta_2(12J)](n_1 - u_1)(n_3 - u_3) = 0, \end{aligned} \tag{7.9a}$$

where

$$\Theta_2(h) \equiv (n_2 - u_2)^2\, \Phi_t(-h) - n_2 z_2 \Phi_t(h). \tag{7.9b}$$

Similar equations follow for u_3 and u_1, i.e., we need to solve M nonlinear coupled equations to obtain u_i, $i = 1, 2, ..., M$. One may prove easily that such a system of equations has the van Beijeren Schulman solution

$$u_i = n_i^2, \qquad i = 1, ..., M, \tag{7.10}$$

when $\Phi_t = \text{const.}$, the later corresponding to the situation with no correlations along each column we discussed before, i.e., to the limit $E \to \infty$.

Step (ii). Consider now transitions from column i to column $i+1$; i.e., the starting configuration is

$$\begin{array}{ll} \text{column } j = & \begin{array}{cccc} i-1 & i & i+1 & i+2 \end{array} \\ \text{occupation variables} & \begin{cases} & \sigma_1 & \sigma_2 & \\ \sigma_3 & 1 & 0 & \sigma_4 \\ & \sigma_5 & \sigma_6 & \end{cases} \end{array}$$

According to Eqs. (7.5) and (7.1), these have a probability given by

$$\begin{aligned} R_i^+(n_{i-1}, n_i, n_{i+1}, n_{i+2}) &= \sum_{\boldsymbol{\sigma}} \prod_j p'(\boldsymbol{\sigma}_j)\, \Phi_h(\beta \delta H) \\ &= \sum_{\boldsymbol{\sigma}_j,\ j = i-1, i, i+1, i+2} p'(\boldsymbol{\sigma}_{i-1})\, p(\boldsymbol{\sigma}_i)\, p(\boldsymbol{\sigma}_{i+1})\, p(\boldsymbol{\sigma}_{i+2})\, \Phi_h(\beta \delta H). \end{aligned} \tag{7.11}$$

where the second equality follows by noticing that δH only depends on $\boldsymbol{\sigma}_j$, $j = i-1$, i, $i+1$, $i+2$, and that $p'(\boldsymbol{\sigma}_i) \equiv \pi_E(\boldsymbol{\sigma}_i; \eta_i; \boldsymbol{\eta})$ is normalized to unity. Moreover, δH

only depends in practice on the occupation variables around the pair affected by the interchange, so that one may define the local probabilities

$$\pi_l(\{\sigma_{ik}; k = l, l+1, \ldots\}) = \sum_{\boldsymbol{\sigma}_l - \{\sigma_{ik}\}} p'(\boldsymbol{\sigma}_l), \tag{7.12}$$

where the sum over all column configurations $\boldsymbol{\sigma}_l$, excluding the spin variables σ_{ik}, $k = l, l+1, \ldots$, to simply write for the situation schematically depicted above that

$$R_i^+ = \sum_{\sigma_1, \ldots, \sigma_6} \pi_{i-1}(\sigma_3)\, \pi_l(\sigma_1, 1, \sigma_5)\, \pi_{i+1}(\sigma_2, 0, \sigma_6)\, \pi_{i+2}(\sigma_4)\, \Phi_h(\beta \delta H), \tag{7.13}$$

where the π's may be computed as before; i.e.,

$$\pi_l(\sigma_l) = \begin{cases} n_l & \text{when} \quad \sigma_l = 1 \\ 1 - n_l & \text{when} \quad \sigma_l = 0 \end{cases} \tag{7.14}$$

for $l = 3$ or 4,

$$\pi_l(\sigma_1, 1, \sigma_5) = n_l^{\,3} u_l^{\sigma_1 + \sigma_5} (n_l - u_l)^{2 - \sigma_1 - \sigma_5} \tag{7.15}$$

and

$$\pi_{l+1}(\sigma_2, 0, \sigma_6) = (1 - n_l)^{3 - \sigma_2 - \sigma_6} v_{l+1}^{\sigma_2 + \sigma_6} (n_{l+1} - u_{l-1})^{\sigma_2 + \sigma_6}; \tag{7.16}$$

here $\sigma_l = 1$ or 0, $l = 1, 2, \ldots, 6$. Equations (7.13)–(7.16), together with the set (7.9) giving $u_l = u_l(\mathbf{n})$ and $u_{l+1} = u_{l+1}(\mathbf{n})$, constitute the solution at this step. When one assumes $E \to \infty$, so that (7.10) holds and takes the function Φ in Eq. (7.13), it follows simply that

$$\begin{aligned} R_i^+ = {} & n_l v_{l+1} (n_{l-1} \alpha^{-1} + v_{l-1} \alpha)(n_{l+2} \alpha + v_{l+2} \alpha^{-1}) \\ & \times (n_l^2 \alpha^{-2} + 2 n_l v_l + v_l^2 \alpha^2)(n_{l+1}^2 \alpha^2 + 2 n_{l+1} v_{l+1} + v_{l+1}^2 \alpha^{-2}), \end{aligned} \tag{7.17}$$

with $\alpha \equiv \exp(\beta J)$, which is precisely the result of van Beijeren and Schulman [7].

Step (iii). According to Eq. (7.5), the densities n_l have N changes of size N^{-1} during a unit time interval. Thus one may use the column height N as a system size parameter Ω to perform an Ω-expansion [38] of the master equation (7.4). This is, as we discussed before, identical to the expansion in the limit $E \to \infty$, so that we only outline the main result here and refer to the paper by Krug *et al.* for most of the details [39].

The average local densities are governed for large N by conservation-type deterministic equations:

$$dn_l/dt = -[J_l(\mathbf{n}) - J_{l-1}(\mathbf{n})] \tag{7.18}$$

with the current between columns i and $i+1$ given by $J_i = R_i^+ - R_{i+1}^-$, where $R_{i+1}^- \equiv R_{i+1}^-(n_{i+2}, n_{i+1}, n_i, n_{i-1})$ represents the number of transitions per unit of time from $i+1$ to i (cf. Eq. (7.11)), and the fluctuations around those averages are governed by Langevin equations

$$d\phi_j/dt = \sum_{l=1}^{M} L_{jl}(\mathbf{n})\, \phi_l + W_j(t), \tag{7.19}$$

where the W_j represent fluctuating Gaussian forces with zero mean and covariance

$$g_{ij} = \sum_l [(\delta_{i,l+1} - \delta_{i,l})(\delta_{j,l+1} - \delta_{j,l})\, R_l^+ + (\delta_{i,l} - \delta_{i,l+1})(\delta_{j,l} - \delta_{j,l+1})\, R_l^-], \tag{7.20}$$

and

$$L_{ij} = -(\delta/\delta n_j)(J_i - J_{i-1}) \tag{7.21}$$

which is obtained by linearizing (7.18) around the solution $\mathbf{n}(t)$.

Correlations

An important difference between the situation here and that for $E \to \infty$ concerns the behavior of the spatial correlations, e.g., as given by the structure function defined as

$$S(\mathbf{k}) = \sum_{\mathbf{r}} e^{i\mathbf{k}\cdot\mathbf{r}} [\langle \sigma_{0,0} \sigma_{j,1} \rangle - \langle \sigma_{0,0} \rangle \langle \sigma_{j,1} \rangle], \tag{7.22}$$

where $\mathbf{k}$ becomes continuous when $N, M \to \infty$, $\mathbf{k} \equiv (k_e, k_\perp)$, $\mathbf{r} \equiv (j, l)$, and

$$\langle \sigma_{j,l} \sigma_{j',l'} \rangle \equiv \sum_{\boldsymbol{\eta}} \pi_E(\boldsymbol{\eta}; t) \sum_{\boldsymbol{\sigma}_l, \boldsymbol{\sigma}_{l'}} \sigma_{j,l} \sigma_{j',l'} \times p_E(\boldsymbol{\sigma}_l, \eta_l; \boldsymbol{\eta})\, p_E(\boldsymbol{\sigma}_{l'}, \eta_{l'}; \boldsymbol{\eta}). \tag{7.23}$$

It follows immediately that

$$\langle \sigma_{j,l} \rangle = \sum_{\boldsymbol{\eta}} \pi_E(\boldsymbol{\eta}; t)\, n_l \equiv \langle n_l \rangle_p \tag{7.24}$$

and that

$$\langle \sigma_{j,l} \sigma_{j',l'} \rangle = \begin{cases} \langle \langle \sigma_{j,l} \sigma_{j',l'} \rangle_n \rangle_p & \text{within each column} \\ \langle n_l n_{l'} \rangle_p & \text{between different columns,} \end{cases} \tag{7.25}$$

where

$$\begin{aligned} \langle \cdots \rangle_n &\equiv \sum_{\boldsymbol{\sigma}_l} P_E(\boldsymbol{\sigma}_l, \eta_l; \boldsymbol{\eta}) \cdots \\ \langle \cdots \rangle_p &= \sum_{\boldsymbol{\eta}} \pi_E(\boldsymbol{\eta}, t). \end{aligned} \tag{7.26}$$

Let us define

$$S_{\perp}(\mathbf{k}) = \sum_{\mathbf{r}} e^{i\mathbf{k}\cdot\mathbf{r}} [\langle n_0 n_j \rangle_p - \langle n_0 \rangle_p \langle n_j \rangle_p]; \tag{7.27}$$

one has then after some algebra that

$$S(\mathbf{k}) = S_{\perp}(\mathbf{k}) + \langle S'(k_{\hat{\mathbf{e}}}) \rangle_p, \tag{7.28}$$

where

$$S'(k_{\hat{\mathbf{e}}}) = \sum_{r} e^{ik_{\hat{\mathbf{e}}} r} [\langle \sigma_{0,0} \sigma_{r,0} \rangle_p - n_0^2]. \tag{7.29}$$

We study the behavior of the first term in Eq. (7.28). The second term could introduce some nonanalyticity in the structure function implying a power law decay behavior in the two body correlation function. The behavior of $S_{\perp}(\mathbf{k})$ is given by an expression *formally* identical to that for the whole structure function in Ref. [8], namely,

$$S_{\perp}(k_{\perp}) = -\frac{\hat{q}(k_{\perp})}{2\hat{L}(k_{\perp})} = \frac{D}{R_{23} + R_{14}(1 + 2\cos k_{\perp})}, \tag{7.30}$$

where $\hat{g}(k_{\perp})$ and $\hat{L}(k_{\perp})$ are respectively the one-dimensional Fourier transforms of (7.20) and (7.21), and we have introduced the notation

$$R_{ij}(n) = [\delta R_i^{+} \delta x_j - \delta R_i^{+} \delta x_i]_{x_i = n} \tag{7.31}$$

and $D(n) = R_2^{+}(x_1, x_2, x_3, x_4)$ when $x_i = n$, $i = 1, 2, 3$, and 4.

Critical Temperature

Summing up, most system properties may be obtained from Eqs. (7.9), (7.13) (7.16), and (7.31) whose solution is just a matter of algebra (actually, a tedious task which can be a alleviated in practice by using a computer package such as REDUCE to manipulate those expressions). As an example, we study here the behavior of the nonequilibrium critical temperature $T_c(E, n)$ in the limit $\Gamma \to \infty$; other macroscopic quantities will be described in Section 9 for the (more general) case of varying Γ.

The critical properties of the system with attractive interactions ($J > 0$) follows from the condition

$$R_{23} + 3R_{14} = 0 \tag{7.32}$$

which make $S(\mathbf{k})$ diverge. The resulting function $T_c(E, n)$ is interesting; cf. Figs. 6 and 7. Indeed, it shows evidence of the existence of a critical density $n_c = 0.152$ separating two different kinds of behaviors for $n \leqslant n_c$ and for $0.5 \geqslant n > n_c$, respectively. Within the latter range, $T_c(E)$ for a given n and increasing values of E first

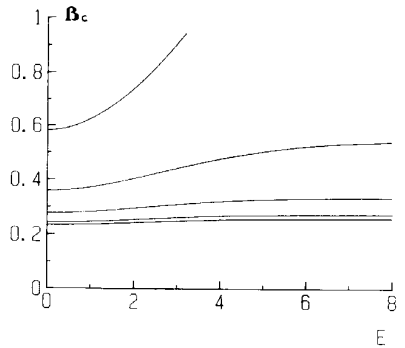

FIG. 6. The nonequilibrium transition temperature, $\beta_c(E) = 1/kT_c(E)$, in the limit $\Gamma \to \infty$ when $J > 0$ for different densities: $n = 0.1$, 0.2, 0.3, 0.4, and 0.5 from top to bottom.

increases by a very small amount for $0 \leqslant E \leqslant 1$ (a fact which is not quite evident on the scale of Fig. 6) and clearly decreases afterwards for $1 \leqslant E \leqslant 5$, the decrease being more pronounced as $n > n_c$ is lowered, and tends finally to an asymptotic finite value $T_c(\infty)$; for a given field, $T_c(E, n)$ decreases with n. When $n < n_c$, however, $T_c(E)$ decreases monotonically with increasing E and tends to zero as $E \to \infty$. That is, the phase segregation is suppressed in the infinite-field limit, and the field tends to destroy (horizontal) correlations in such a way that $T_c(E) < T_c(0)$ in the limit

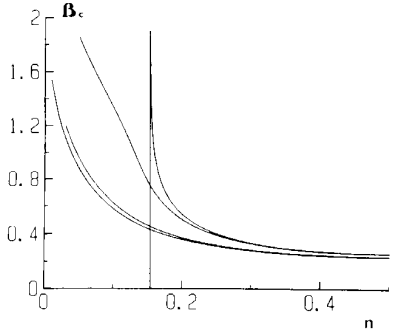

FIG. 7. The quantity β_c in Fig. 6 is plotted here versus n for different values of the field: $E = 500$, 5, 1, and 0 from top to bottom.

TABLE I

Some Representative Values of $T_c(E)$ for the Model in Sections 7 and 8

	$T_c(E=\infty)$	$T_c(E=0)$	
n	(a) and (c)	(a) and (b)	(c)
0.1	0	1.719	0
0.2	1.847	2.792	0
0.3	3.000	3.610	1.399
0.4	3.648	4.110	2.732
0.5	3.861	4.277	3.090

Note. (a) $\Gamma \to \infty$ and $J>0$, (b) $\Gamma \to 0$ and $J>0$, (c) $\Gamma \to \infty$ with $J<0$ along the field and $J>0$ perpendicular to the field. Notice that $T_c(E=\infty)$ is the same for (a) and (c); i.e., the horizontal interactions are irrelevant when $E \to \infty$ *and* $\Gamma \to \infty$, and that the equilibrium critical temperature of the model is independent of the values for Γ, as expected; also, $T_c(E=\infty, n)=0$ independent of n for case (b).

$\Gamma \to \infty$; the fact that this behavior is opposite in a sense to the one when $\Gamma \approx 1$ (cf. Section 9 and Ref. [5]), where $T_c(E) > T_c(0)$, highlights the effect of the parameter Γ. Table I lists some numerical values for $T_c(E, n)$.

The critical behavior when the interactions are repulsive ($J<0$) is to be associated with the condition

$$R_{23} - R_{14} = 0. \tag{7.33}$$

This reveals no phase transition for any value of E and n, a fact which is already known to hold [8] in the limit $E \to \infty$.

8. The Slow Rate Limit

The model and method of solution in Sections 6 and 7 allows the consideration of arbitrary transition probabilities for the two principal directions of the lattice, a possibility which is not contained in the previous formulations for $E \to \infty$ [7, 8]. It thus seems interesting to consider the case $\Gamma \to 0$, where one greatly speeds up a priori the transitions perpendicular to the field and the anisotropic case with horizontal ferromagnetic interactions and vertical antiferromagnetic ones, for instance.

The slow rate limit $\Gamma \to 0$ simply follows from above when one replaces the functions Φ_v in Eq. (7.8) and Φ_h in Eq. (7.11) by Φ_h and Φ_v, respectively, where $\Phi_h = \Phi(\delta H)$ and $\Phi_v = \Phi(\delta H, E)$ in accordance with Eqs. (6.1) and (2.3). The resulting behavior for $T_c(E)$ is illustrated by Figs. 8 and 9 and by Table I in the case of attractive interactions. That is, $T_c(E)$ decreases monotonically with increasing E, so

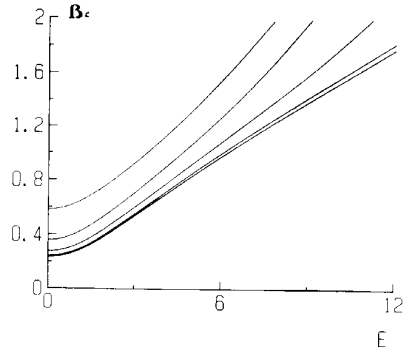

FIG. 8. Same as Fig. 6 but for $\Gamma \to 0$.

that $T_c(\infty)=0$, for all values of the density n, and $d^2T_c(E)/dE^2$ apparently changes sign around $E=5$ when n is large enough, this probably reflecting that both cases, $\Gamma \to \infty$ and $\Gamma \to 0$, have the same stationary state (the particular equilibrium state for the model) in the limit $E \to 0$. The system with $E \to \infty$ and $\Gamma \to 0$ may thus be viewed as a collection of rows, each in a steady state with respect to the equilibrium transition probability at temperature T, which are independent except for the fact that they interchange particles at random, i.e., independently of temperature, thus avoiding any long range order. It also seems noticeable that the asymptotic

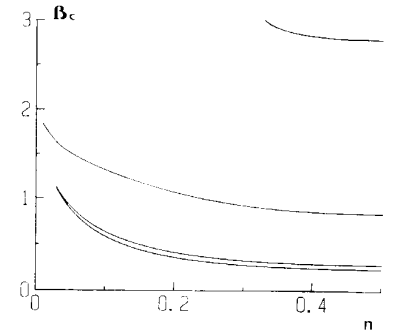

FIG. 9. Same as Fig. 7 except that $\Gamma \to 0$ and $E = 20$, 5, 1, and 0 from top to bottom.

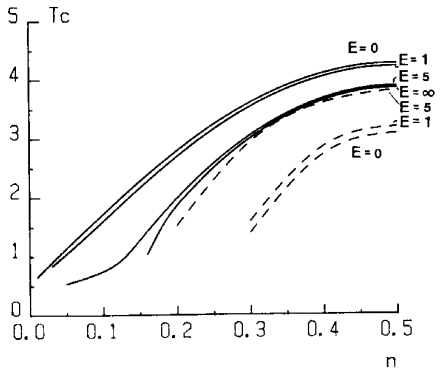

FIG. 10. The transition temperature as a function of density in the limit $\Gamma \to \infty$ for several representative values of the field, for the ferromagnetic case considered in Figs. 6 and 7 (solid lines) and for the case where the interactions along the field are antiferromagnetic and those in the perpendicular direction are ferromagnetic (dashed lines); the behavior for $E = \infty$ is the same for both cases.

behavior in Fig. 8 can be fitted by $T_c(E)^{-1} = a + bE$, where b decreases with increasing n and a is very small.

The case $\Gamma \to 0$ with repulsive interactions shows no phase segregation for any value of E and n, as for $\Gamma \to \infty$. It thus seems interesting to introduce further anisotropies in the model by allowing different kinds of interactions for the two principal directions of the lattice. It follows, for instance, that the phase segregation is also suppressed in the limit $\Gamma \to \infty$, independently of the values of E and n, when one introduces attractive interactions along the field direction and horizontal repulsive ones, while long range order is possible when the vertical interactions are repulsive and the horizontal interactions are attractive. The latter case is illustrated by Fig. 10, revealing that $T_c(E)$ increases with E for $n \gtrsim 0.3$ until it reaches a finite asymptotic value $T_c(\infty)$, $T_c(E) = 0$ for small fields within the range $0.152 = n_c < n \lesssim 0.2$, and $T_c(E) = 0$ for any E when $n < n_c$; in any case, $T_c(E, n)$ is the same here as for the case where all the interactions are attractive. Figure 10 also includes an interesting comparison between those two cases; such a comparison reveals the relevant role played by the parameter n and by the sign of the interactions.

9. FULL TWO-DIMENSIONAL BEHAVIOR

While the models discussed in Sections 7 and 8 exhibit non-trivial two-dimensional spatial structure, the limiting conditions $\Gamma \to \infty$ or $\Gamma \to 0$, cause them to

approximate, as E becomes larger, quasi-one-dimensional systems. That is, those models may describe a crossover from $d = 2$ to $d = 1$ (which also bears some practical interest) but, in order to obtain the full two-dimensional behavior of the DDS which can be compared to most experimental and Monte Carlo data, one needs to consider systems with general E, $\Gamma \in [0, \infty]$.

An approach to the behavior of the DDS may be based on the observation from Monte Carlo simulations (cf. (c) in Section 6), that the low-temperature nonequilibrium steady states are as in Fig. 5. That is, we shall assume that a system with density n and temperature $T < T_c(E)$ can be divided into two (coexisting) homogeneous phases of densities $n_L = n_L(T, E)$ and $n_G = n_G(T, E)$, respectively, with $1 \geq n_L \geq n_G \geq 0$ for all T and E, $n_L(T = 0, E) = 1$ and $n_G(T = 0, E) = 0$ for all E, and

$$n_L(T, E) = n_G(T, E) = n, \qquad T > T_c(E) \qquad \text{for all } E; \tag{9.1}$$

the latter may be taken to define $T_c(E)$. Moreover, it is assumed that the two homogeneous phases are separated by a single well-defined interface parallel to the field direction, where the density changes discontinuously from n_L to n_G, and that there are particle currents between them which only depend on the global properties of the two phases. This, together with the extra assumption that the phases immediately stabilize to the new value of the density after each horizontal transition, allows one to describe the system by means of two connected (kinetic) cluster-variation equations, one for each coexisting homogeneous phase. Our objective also requires that we distinguish explicitly between the two principal directions within each phase.

Consider a homogeneous phase with density n and temperature T, under the action of a field $E\hat{\mathbf{e}}$, which involves as a consequence of the (anisotropic) transition probability (6.1), i.e., $c_{\hat{\mathbf{e}}} = w_{\parallel}(\delta H, E)$ along the vertical direction and $c_{\hat{\mathbf{e}}} = w_{\perp}(\delta H)$ along the horizontal direction; let us denote by $u_{\parallel}$ and $u_{\perp}$ the respective densities of n.n. pairs of particles. These satisfy kinetic equations which are similar to Eq. (4.3), except that one now needs to allow the transition rates to depend on the orientation relative to the field. It is convenient to refer to the clusters represented before Eqs. (7.6) and (7.11), and to write $N_i^{+} = N_i' + N_i''$, where $i = 1, 2$, $N_1' = \sigma_3$, $N_2' = \sigma_4$, $N_1'' = \sigma_1 + \sigma_5$, and $N_2'' = \sigma_2 + \sigma_6$, for the number of particles in D_i (cf. Section 4). Therefore,

$$\frac{du_{\parallel}}{dt} = \sum_{N_1', N_2' = 0}^{1} \sum_{N_1'', N_2'' = 0}^{2} [(N_2' - N_1')\, w_{\perp}(\delta H)\, Q^{+}_{N_1' N_2' N_1'' N_2''}(u_{\perp}, u_{\parallel}) + (N_2'' - N_1'')\, w_{\parallel}(\delta H, E)\, Q^{\parallel}_{N_1' N_2' N_1'' N_2''}(u_{\perp}, u_{\parallel})], \tag{9.2}$$

where $\delta H = 4J(N_1^{+} - N_2^{+})$, and $Q^{\perp}$ and $Q^{\parallel}$ are defined as in Eq. (4.1), except that they refer now to the local clusters shown before Eq. (7.6), where the transition

occurs in the direction of the field, and before Eq. (7.11), where the transition is orthogonal to the field. That is, one has that

$$Q^{\perp}_{+\,-N_1^{+}N_2^{+}N_1^{-}N_2^{-}}(u_{\perp},u_{\parallel})=\begin{bmatrix}2\\N_1''\end{bmatrix}\begin{bmatrix}2\\N_2''\end{bmatrix}u_{\perp}^{N_1'}\times z_{\perp}^{1\,-\,N_2'}[\tilde{n}(1-\tilde{n})]^{-3}\,u_{\parallel}^{N_1''}z_{\parallel}^{2-N_2''}[\tfrac{1}{2}(1-u_{\perp}-z_{\perp})]^{2-N_1'+N_2'}\times[\tfrac{1}{2}(1-u_{\parallel}-z_{\parallel})]^{2-N_1''+N_2''},\tag{9.3a}$$

with $z_{\perp(\parallel)}=1-2\tilde{n}+u_{\perp(\parallel)}$, and

$$\begin{aligned}Q^{\perp}_{\;+\,N_2^{+}N_1^{+}N_2^{-}N_1^{-}}(u_{-},u_{\parallel})&=Q^{\perp}_{+\;\;N_1^{+}N_2^{-}N_1^{-}N_2^{+}}(u_{-},u_{\parallel})\\ Q^{\parallel}_{+\;\;N_1^{+}N_2^{-}N_1^{-}N_2^{+}}(u_{\perp},u_{\parallel})&=Q^{\perp}_{+\,-N_1^{+}N_2^{-}N_1^{-}N_2^{+}}(u_{\parallel},u_{-}).\end{aligned}\tag{9.3b}$$

Those two equations for $du_{\perp(\parallel)}/dt$ constitute our basic description of a homogeneous (anisotropic) phase, either the liquid phase with $\tilde{n}=n_L$, $u_{\parallel}=u_{\parallel}^{L}$, and $u_{\perp}=u_{\perp}^{L}$, or the gas phase at the same temperature with $\tilde{n}=n_G$, $u_{\parallel}=u_{\parallel}^{G}$, and $u_{\perp}=u_{\perp}^{G}$. The phases are then related by writing

$$dn_L/dt=j_{G\to L}-j_{L\to G},\tag{9.4}$$

where it will be assumed that the number of particles crossing the interface per unit time from the liquid (gas) to the gas (liquid) phase equals the probability for the average local configuration of the interface times the corresponding probability per unit time. That is,

$$j_{L\to G}=Q_{LG}(n_L,n_G)\,w_{\perp}(\delta\mathbf{H}_{LG}),\tag{9.5}$$

and a similar expression for $j_{G\to L}$, where $\delta\mathbf{H}_{LG}=12J(n_L-n_G)$,

$$Q_{LG}(n_L,n_G)=[n_L(1-n_G)]^{-2}\,(u_{\perp}^{L})^{n_L}\,(u_{\parallel}^{L})^{2n_L}\times[\tfrac{1}{2}(1-2n_L+u_{\perp}^{L})]^{1\,-\,n_L}\,[\tfrac{1}{2}(1-2n_L+u_{\parallel}^{L})]^{2(1-n_L)}\,(z_{\perp}^{G})^{1\,-\,n_G}\times[\tfrac{1}{2}(1-2n_G+u_{\perp}^{G})]^{1-n_G}\,(z_{\parallel}^{G})^{2(1-n_G)}\,[\tfrac{1}{2}(1-2n_G+u_{\parallel}^{G})]^{2(1\;\;n_G)},\tag{9.6}$$

and

$$Q_{GL}(n_G,n_L)=Q_{LG}(n_G,n_L).\tag{9.7}$$

That probability refers to the average local configuration:

LIQUID			GAS		
	*		*		
n_L	*	σ_1	σ_2	*	n_G
	*		*		

assuming that σ_1 is surrounded by $3n_L$ particles within the liquid phase and that σ_2 is surrounded by $3n_G$ particles within the gas phase, and taking $\sigma_1=1$, $\sigma_2=0$ for $j_L\to j_G$. We shall consider explicitly in the following the ferromagnetic case with the Metropolis rates (2.4), i.e.,

$$w_{\parallel}=\tfrac{1}{2}(1-p)[\Phi_{\parallel}^{+}+\Phi_{\parallel}^{-}],\tag{9.8}$$

where $p\equiv(1+\Gamma)^{-1}$ and

$$\Phi_{\parallel}^{\pm}=\begin{cases}\exp(-\beta\delta H\pm E), & \text{when}\quad -\beta\delta H\pm E\leqslant 0\\ 1, & \text{otherwise}\end{cases}\tag{9.9}$$

and

$$w_{\perp}=\begin{cases}p\cdot\exp(-\beta\delta H), & \text{when}\quad \delta H\geqslant 0\\ p, & \text{otherwise,}\end{cases}\tag{9.10}$$

which is the one closer to the case studied before via Monte Carlo (MC) methods [4–6], and global densities $n=\frac{1}{2}$ and 0.1.

Critical Density, $\Gamma=1$

The behavior of the order parameter, $m\equiv n_L-n_G$, for the most interesting case of $n=\frac{1}{2}$ and $p=\frac{1}{2}$ (i.e., $\Gamma=1$) is depicted in Fig. 11. This reveals, in particular, that $T_c(E)$ is an increasing function of E, in accordance with MC simulations [5]. Such a behavior may be understood by noticing that the external field E induces two

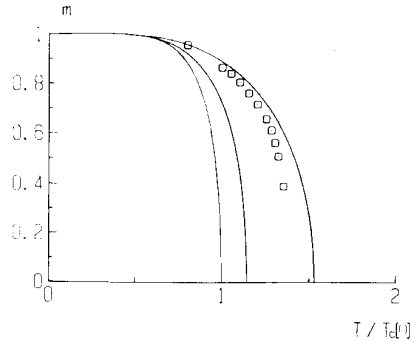

FIG. 11. The order parameter $m\equiv n_L-n_G$ for the two-dimensional DDS in Section 9 when $n=\frac{1}{2}$, $E=0$, 1, and ∞ (from left to right), and $p\equiv(1+\Gamma)^{-1}=\frac{1}{2}$. The circles represent some MC data [5] for $E=\infty$, $n=\frac{1}{2}$, $\Gamma=1$, and $L\to\infty$.

competing effects on the system correlations: (i) The field produces strip-like configurations; i.e., it enhances long-ranged correlations and, consequently, it tends to increase T_c, but (ii) it also destroys local, short-ranged correlations within the strips, which causes T_c to decrease. Thus, it seems that the (anisotropic) effect (i) dominates over the more local (ii) in the present case of ferromagnetic interactions, while one should expect (ii), which effectively destroys local order, to dominate over (i) when the interactions are antiferromagnetic; the latter expectation seems consistent with the results of MC computation in Ref. [2].

The nonequilibrium critical temperature of the model when $E \to \infty$ is $T_c(\infty) = 1.530\, T_c(0)$, to be compared with the MC result $T_c(\infty) \approx 1.355\, T_c(0)$. This and other differences in Fig. 11 between our curve $m = m(T)$ and the one obtained via the MC method can be interpreted as a consequence of the fact that our model involves a mean-field assumption, so that it overestimates long-ranged correlations and, consequently, it presents an order which is more stable against thermal fluctuations than the one characterizing the MC model. We also find a critical behavior $m \approx [1 - T/T_c(E)]^{\beta}$, $\beta = \frac{1}{2}$, as expected, while the MC result is $\beta \approx 0.23$.

The energy density is $e = -4Ju$ where, for the present case $n = \frac{1}{2}(u_L + u_G)$, where $u_{L(G)}$ is the density of pairs of particles in the liquid (gas) phase,

$$u_{L(G)} = \tfrac{1}{2}(u_{\perp}^{L(G)} + u_{||}^{L(G)}); \tag{9.11}$$

$u_{\perp}^{L(G)}$ and $u_{||}^{L(G)}$ are the stationary solutions of Eqs. (9.2)–(9.7). Figure 12 depicts the behavior of e/e_0, $e_0 \equiv -2J$, and Fig. 13 that of $e_{L(G)}/e_0 \equiv u_{L(G)}$. Figure 12 reveals

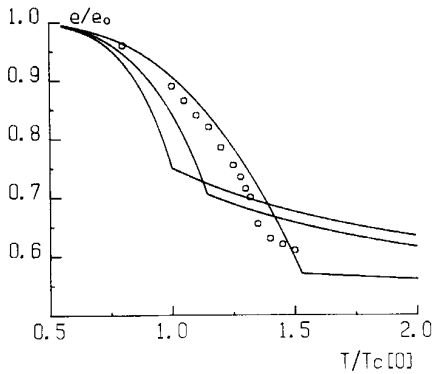

FIG. 12. The energy density normalized to $e_0 \equiv -2J$ versus temperature when $n = \frac{1}{2}$, $p = \frac{1}{2}$, and (from left to right) $E = 0$, 1, and ∞. The circles represent the MC data [5] for $E = \infty$, $n = \frac{1}{2}$, $\Gamma = 1$, and $L \to \infty$.

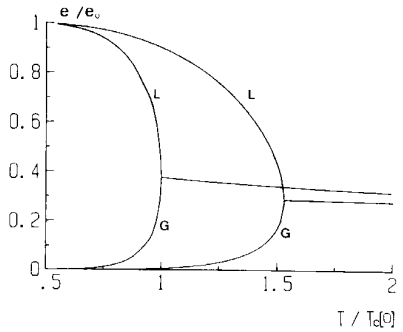

FIG. 13. The energy density for liquid, e_L, and gas, e_G, phases (as indicated) for $n = \frac{1}{2}$, $p = \frac{1}{2}$, and $E = \infty$ (right curve); $e_L = e_G$ for $T > T_c(E)$.

that $e(T)$ decreases with increasing E for any given $T \geqslant T_c(E)$, while $e(T)$ increases with E when $T < T_c(E)$; that is, the field effectively condenses the particles below $T_c(E)$, while it acts as a dispersing agent above $T_c(E)$. Figure 13 provides similar information concerning each phase.

It is convenient to introduce a *parameter of local anisotropy* defined as

$$\mu \equiv N_{\perp}^{++}/N_{||}^{++}, \tag{9.12}$$

where $N_{\perp(||)}^{++}$ is the number of pairs of particles along the horizontal (vertical) direction. Figure 14 indicates that $\mu = 1$, independent of T, for the isotropic system

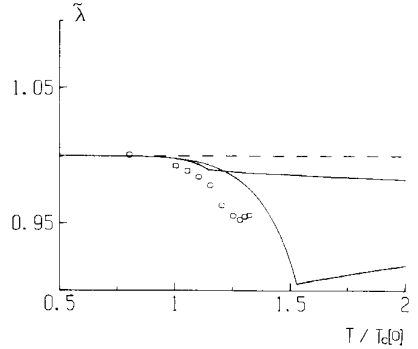

FIG. 14. The parameter μ defined in (9.12) for $n = \frac{1}{2}$, $p = \frac{1}{2}$. The dashed line is for $E = 0$, the solid lines are for $E = 1$ (a) and ∞ (b), the circles are MC data for $E = \infty$, $L \to \infty$.

$E=0$, while any field produces anisotropic clusters, the anisotropy being more important at any T as E is increased. Also, μ always decreases monotonically with increasing T when $T<T_c(E)$, while it exhibits different qualitative behaviors above $T_c(E)$ for small and large values of E. This may be understood as follows: At $T=0$, the system is fully condensed and locally isotropic; any finite $T<T_c(E)$, however, allows a particle current along the field direction, and anisotropic clusters form, the anisotropy increasing as T is increased. When $T>T_c(E)$ and the field is very large, μ increases monotonically with T from the minimum $\mu_c \equiv \mu[T_c(E)]$; i.e., the anisotropy decreases revealing that clusters are relatively unstable against the actions of field and thermal fluctuations. When the field is smaller the thermal fluctuations are not helped so efficiently by the field in destroying local order (cf. the first paragraph in the present subsection), but the field tends to induce a higher anisotropy as the particles mobility increases, when T becomes higher. Regardless of the magnitude of the field, μ tends towards an asymptotic value μ_∞ as $T\to\infty$, which decreases with increasing E. This kind of local anisotropic order above $T_c(E)$, a nonequilibrium effect which was observed originally in MC simulations [5], is known to induce a power law decay of correlations in the high temperature phase [42].

Also interesting is the study of the *short-ranged order parameter* defined as

$$\sigma \equiv (1-u)^{-2}[\tfrac{1}{4}(1+u)^2 - m^2] \tag{9.13}$$

(or, alternatively in some circumstances [40], as $N^{++}/(N^{+-})^2$). This quantity turns out to be very helpful in analyzing phase transition, because it always remains finite at T_c (excluding the case $T_c=0$) and presents qualitatively different behaviors associated with different values for the critical exponents [40]. For instance, if the exponents take the classical values $\beta=\frac{1}{2}$, $\alpha=0$, then σ decreases monotonically with increasing T, while any other set of values for β and α yields a finite peak in $\sigma(T)$ at T_c [40]. Consequently, the situation depicted by Fig. 15 reveals that the present analysis yields classical critical behavior for any value of E, as expected, while it also reveals that the MC data for $\Gamma=1$ [5] is characterized by nonclassical exponents, unlike the case $\Gamma\to\infty$ [7, 8, 4] and other nonequilibrium situations [1].

The electric field induces a particle current. This current defined as in Eq. (5.16) with $\hat{\mathbf{x}}$ indicating the direction of the field, is represented by Fig. 16. The main novel result here is that, as is found in experiments and MC simulations for $d\geq 2$ [2–6], but not for the case $d=1$ considered in Section 5, the slope of the current-versus temperature curve changes discontinuously at $T_c(E)$.

Off-Critical Density, $\Gamma=1$

Off-critical densities ($n\neq\frac{1}{2}$) have only been studied before in the limit $\Gamma\to\infty$ [7, 8] and by MC methods when $\Gamma=1$ [6]. The latter suggested that the phase transition remains second order for $\frac{1}{2}\geq n\geq 0.35$ while it becomes discontinuous when $0.2\geq n$; Fig. 17 confirms the existence of a first-order phase transition in the

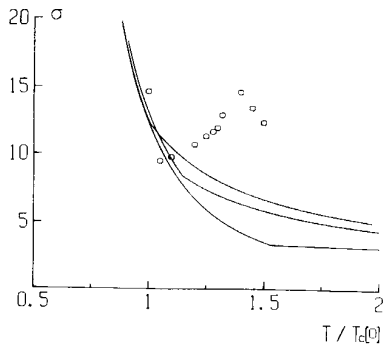

FIG. 15. The parameter σ defined in (9.13) for $n=\frac{1}{2}$, $p=\frac{1}{2}$, and (from top to bottom) $E=0$, 1, ∞; the circles are MC data for $E=\infty$, $L\to\infty$.

model for small values of n. The same conclusion follows from the behavior of the energy (Figs. 18 and 19) which is now given by

$$e/e_0 = u_L + (1-n)\,n^{-1}u_G. \tag{9.14}$$

The behavior of the short-ranged order parameter (9.13) is represented by Fig. 20, and that of the particle current by Fig. 21. Figures 18–21 have a simple interpretation which requires no further comments.

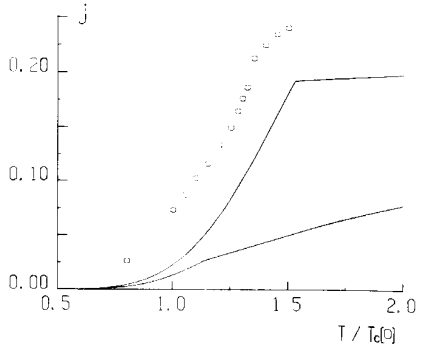

FIG. 16. The particle current (5.16) for $n=\frac{1}{2}$, $p=\frac{1}{2}$, and (from top to bottom) $E=\infty$, 1; the circles are MC data for $E=\infty$, $L\to\infty$ [5].

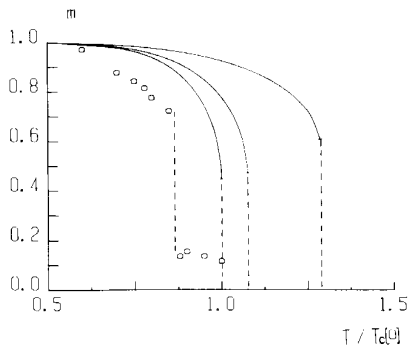

FIG. 17. The order parameter $m \equiv n_L - n_G$ for $n = 0.1$, $p = \frac{1}{2}$, and (from left to right) $E = 0$, 1, and ∞; the circles are MC data for $E = \infty$ and $L = 50$ [6].

Metastability

It should be emphasized that the approximation employed in this section is based on the assumption that the system will order into a single strip below $T_c(E)$. Nevertheless, one may formulate a similar model by assuming instead that the liquid phase consists of several strips, separated by gas strips, oriented along the field direction. As a matter of fact, MC simulations [5, 6] revealed that such states

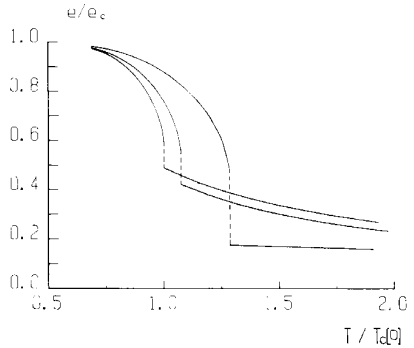

FIG. 18. The energy density (9.14) for $p = \frac{1}{2}$, $n = 0.1$, and (from left to right) $E = 0$, 1, and ∞.

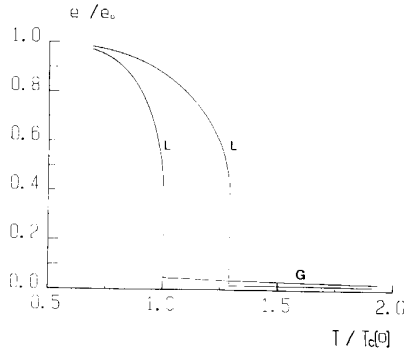

FIG. 19. The energy density for liquid, e_L, and gas, e_G, phases (as indicated) for $n = 0.1$, $p = \frac{1}{2}$, and (from left to right) $E = 0$, ∞.

with several strips usually form at an early stage of the system evolution and may last during extremely large evolutions in most experiments. It thus seems interesting to notice that our formalism allows us to prove that those states with several (or many) strips are metastable and not real stationary states; i.e., they will always decay asymptotically towards a single-strip state, though the relaxation time may be vary large, and they should also be observable in real experiments. This may be

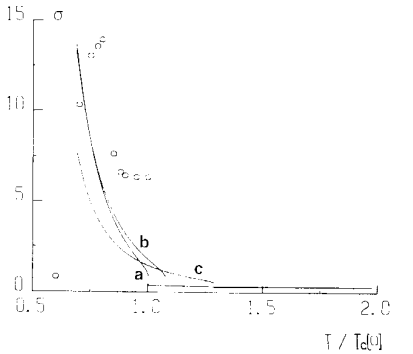

FIG. 20. The parameter σ (9.13) for $n = 0.1$, $p = \frac{1}{2}$, and $E = 0$ (a), 1 (b) and ∞ (c); the circles represent MC data for $E = \infty$ and $L = 50$.

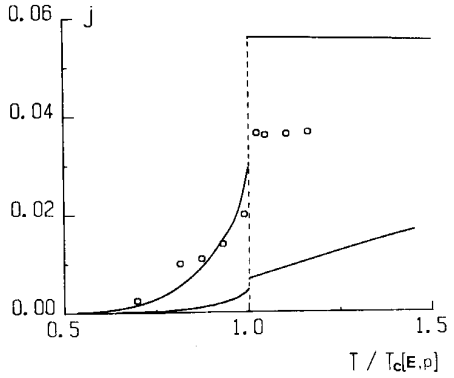

FIG. 21. The particle current (5.16) for $n = 0.1$, $p = \frac{1}{2}$, and (from top to bottom) $E = \infty$ and 1; the circles are MC data for $E = \infty$ and $L = 50$ [6].

proved either by treating numerically a set of coupled kinetic-cluster-variation equations for a system with several strips, which may be written straightforwardly by following the method before, or else, less rigorously, by means of the following simple argument.

Consider a rectangular lattice, $L \times N$, which is half filled with particles driven along the direction with length N. Suppose that the stationary state at low enough temperatures consists of s identical liquid strips separated from each other by gas strips, each having a width $l = L/2s$. The total system energy is

$$E = -4JN \sum_{i=1}^{s} \{l(u_{2i} + u_{2i-1}) - a(T)[(1 - n_{2i-1}) + (1 - n_{2i+1})]\}, \qquad (9.15)$$

where $2s + 1 \equiv 1$, n_{2i} (n_{2i+1}) and u_{2i} (u_{2i+1}) represent respectively the density of particles and that of $++$ pairs in the $2i$th ($(2i \pm 1)$th liquid (gas) strip; the first two terms represent respectively the energy within the liquid and gas strips, and the last term (where we do not need to make explicit the function $a(T) \geqslant 0$, $a(T \to \infty) = 1$) refers to the interface. Then, we may define

$$n_G = s^{-1} \sum_{i=1}^{s} n_{2i-1}, \qquad u_{L,G} = (2s)^{-1} \sum_{i=1}^{s} u_{2i,2i-1} \qquad (9.16)$$

to write

$$e = -4J[u_L + u_G - 2a(T)(1 - n_G) L^{-1} s] \qquad (9.17)$$

for the energy per lattice site, $e \equiv E/NL$. Thus, assuming that u_L, u_G, n_G, and $a(T)$ are independent of s, which is supported by the MC simulations, any variation from the state with s strips is such that

$$\delta e/\delta t = 8Ja(T)(1 - n_G) L^{-1}(\delta s/\delta t). \qquad (9.18)$$

That is, the system search for the lowest energy compatible with the existing constrains guaranties that s will decrease with no apparent lower bound other than $s = 1$, where the system will become real stationary with respect to all dynamical processes.

Varying Values of Γ

The model in this section permits study of the interesting case of varying values of $p \equiv (1 + \Gamma)^{-1} \in [0, 1]$:

The behavior of the order parameter m with p is depicted by Fig. 22 when $n = \frac{1}{2}$, and by Fig. 23 when $n = 0.1$. As expected, m is more sensitive to the effect of the field as p becomes smaller, i.e., when the transitions along the field direction become more frequent (notice that $p = 1$ makes $w_{\uparrow\downarrow} = 0$, cf. Eq. (9.8), so that the parameter E becomes then irrelevant). It is also noticeable that the curves for different values of p (e.g., $p = \frac{1}{2}$ and $p = 0$) tend to lie closer to each other as E is lowered from $E = \infty$, the case represented by Fig. 22. Otherwise, the behavior of m is qualitatively similar for all values of p, and one has that

$$m \approx A(E, p)[1 - T/T_c(E, p)]^{\beta}, \qquad (9.19)$$

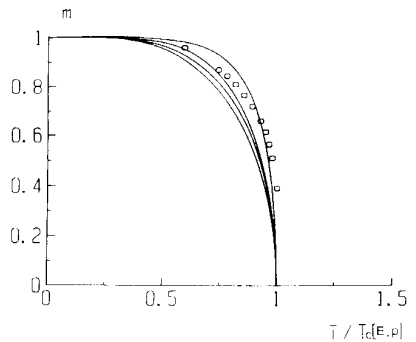

FIG. 22. The order parameter m for $n = \frac{1}{2}$, $E = \infty$, and (from left to right) $p = 1$, 0.9, 0.5, and 0. The behavior for small fields is qualitatively similar, but the curves for different values of p, e.g., $p = \frac{1}{2}$ and $p = 0$, tend to lie closer to each other as E is lowered. The circles represent the MC data for $p = \frac{1}{2}$ [5].

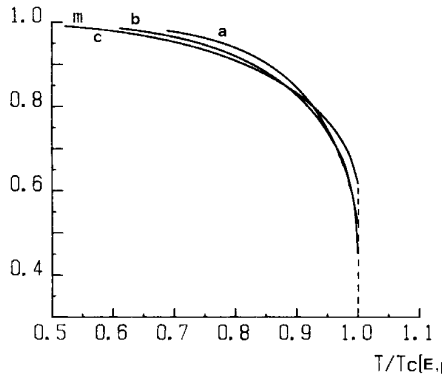

FIG. 23. The order parameter m for $n = 0.1$ for different values of E and p as follows: (a) $p = 1$; (b) $E = 1$, $p = 0$; (c) $E = \infty$, $p = 0$.

with $\beta = \frac{1}{2}$ for all E and p, where the thermodynamic amplitude $A(E, p)$ increases with p (except at $E = 0$) and decreases with E (except at $p = 1$). Concerning Fig. 23, it reveals that the transition is first order for any value of p, and that the value of m at the transition point, m_c, satisfies $m_c(E, p) > m_c(E', p')$ when $p > p'$ and/or $E > E'$. These predictions are very similar to the behavior observed in MC simulations.

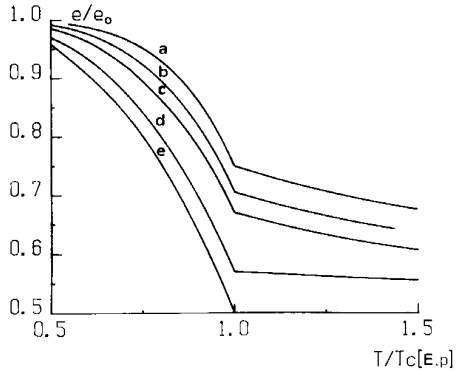

FIG. 24. The energy density as a function of temperature for $n = \frac{1}{2}$: (a) $p = 1$; (b) $E = 1$, $p = \frac{1}{2}$; (c) $E = 1$, $p = 0$; (d) $E = \infty$, $p = \frac{1}{2}$; and (e) $E = \infty$, $p = 0$.

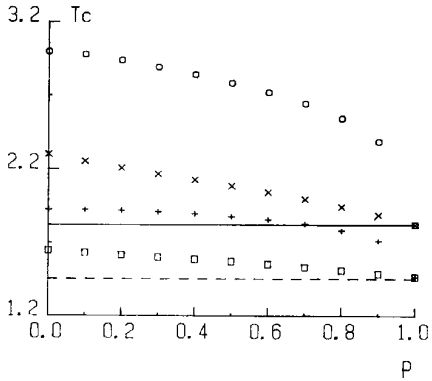

FIG. 25. The transition temperature T_c as a function of p for different values of n and E as follows: (solid line) $n = \frac{1}{2}$, $E = 0$; ($\times$) $n = \frac{1}{2}$, $E = 1$; (○) $n = \frac{1}{2}$, $E = \infty$; (dashed line) $n = 0.1$, $E = 0$; (□) $n = 0.1$, $E = 1$; (+) $n = 0.1$, $E = \infty$.

The current and the energy density (Fig. 24) also behave qualitatively similarly for all values of p. It is noticeable however that $e(T)$ is a constant for $T > T_c$ when $E = \infty$ and $p = 0$. This effect, which was already noted by Krug *et al.* [8], reflects the great influence of the interface in the system behavior, specially in the limiting case $E \to \infty$, $\Gamma \to \infty$. This and other properties of the interface have been investigated recently [41] providing further support for our assumption of a well-defined, flat interface in most circumstances. Concerning the electric current, it is noticeable the fact $j(T)$ decreases with increasing p and tends to disappear as $p \to 1$, as one may expect intuitively.

Finally, we comment on the behavior of the transition temperature with n, E, and p. This is represented by Fig. 25 where one observes in particular that T_c decreases with increasing p for all given values of $E > 0$ and n. This behavior with p is opposite to the observation in a series of MC experiments for $n = \frac{1}{2}$ and $E = \infty$ [4]; we interpret such a disagreement as a consequence of the specific treatment given in this section to the system interface.

10. STABILITY OF THE HIGH-T PHASE

The approach described above is complemented by a mean-field theory for the two-dimensional DDS introduced recently by Dickman [11], which is based on the vanishing of the diffusion coefficient at the critical point. The diffusion coefficient is

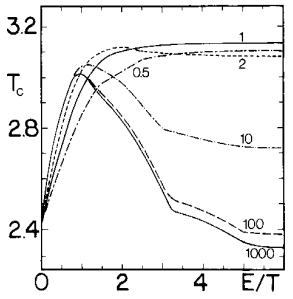

FIG. 26

determined by examining the current in response to a small density gradient, and the calculation proceeds in two steps (see Ref. [11] for further details):

First, the set (9.2)–(9.7) of kinetic equations for cluster densities reflecting nonequilibrium dynamics under the action of the driving field, is integrated at the critical density $n = \frac{1}{2}$ to find the spatially homogeneous steady state given by Eq. (9.1). The stability of this state is then tested by imposing a weak (typically, one part in 10^6) density gradient. Since MC simulations always show the interface oriented along the driving field, the gradient is imposed transverse to the field. Note that this approach is sensitive only to a *local* instability of the homogeneous phase and cannot detect a *first-order* transition. This is not a problem in the present context, since simulations at the critical density always yield a continuous transition. The

TABLE II

Effect of the Parameter Γ on the Critical Temperature, $T_c(E, \Gamma)$, in the Large-Field Limit for the Model in Section 10

	$T_c(\infty, \Gamma)/T_c(0)$	
Γ	MC	MFT
1	1.33 ± 0.02	1.3806
5	1.18 ± 0.02	1.2775
20	1.05 ± 0.01	1.1302
80	1.0	1.0546

Note. $T_c(0)$ is the equilibrium Onsager critical temperature. MC values from Monte Carlo results in Ref. [4], MFT values from mean field theory for square clusters.

homogeneous state becomes unstable at the critical temperature $T_c(E)$. Applying this scheme for the case $\Gamma = 1$ and $E \to \infty$ in the two-dimensional case, one obtains [11] the critical temperatures: $T_c = 3.206$ at the pair approximation level and $T_c = 3.134$ in the square approximation, as compared with the simulation result $T_c = 3.075 \pm 0.007$ [4]. For $d = 3$, the pair approximation yields a critical temperature which agrees with the simulation result, $T_c = 4.83$, to within uncertainty.

The same approach may has been used to obtain new results for different values of Γ. The main findings are summarized in Fig. 26, which shows $T_c(E, \Gamma)$ versus E/T, for several choices of Γ. One observes in particular that while $T_c(E, 1)$ is a monotonically increasing function of E, for $\Gamma > 1$ the critical temperature exhibits a maximum, located at E/T around 1.5. For large driving fields, the effect of increasing Γ is to reduce the critical temperature. The same behavior is observed in simulations, as is shown in Table II.

11. CONCLUSION

We present and discuss a general method for studying lattice models whose time evolution is governed by master equations. It has the philosophy of a "cluster variation" method, i.e., it involves mean-field type assumptions and permits to approach the exact solution of the model with increasing cluster size. This produces an explicit description of the time evolution, steady states, and stability conditions for systems evolving via rather general dynamical processes, e.g., one may study situations in wich a system is affected by external agents leading asymptotically to nonequilibrium steady states. As a consequence, the method can be applied to a large variety of physically interesting situations.

The method is illustrated here in the case of a lattice gas model evolving via nn interchanges which occur under the action of both a thermal bath at inverse temperature $\beta = 1/k_B T$ and a uniform external electric field **E**. The field, along one of the principal lattice directions, induces a net current of particles in some occasions. Such driven diffusive systems (DDS) bears a great theoretical interest, e.g., to investigate nonequilibrium phenomena such as electrical conductivity and far-from-equilibrium phase segregation, when trying to understand nonequilibrium ensembles and universality classes, etc.; DDS are also of practical interest as models of some materials with technological applications.

We considered explicitly several approximations namely: (1) A one-dimensional system solved by the kinetic cluster variation method. (2) A two-dimensional system, whose anisotropy is enhanced by introducing an extra parameter Γ which speeds up the transitions in the direction of the field as compared to those perpendicular to it, in the limiting cases $\Gamma \to \infty$ and 0. This also generalizes the models by van Beijeren and Schulman and by Krug *et al.* ($\Gamma \to \infty$) in that it includes the cases of arbitrary transition probabilities and finite values of E. The model is solved by means of the kinetic cluster variation method, and by using van Kampen's Ω-expansion technique. (3) A mean field solution for the general two-dimensional

system is derived, based on the assumption that below T_c, there is a well-defined interface oriented along the field. That is, the system consists of a homogeneous particle-rich strip of density $n_L = n_L(T, E)$ along the field direction and a homogeneous particle-poor gas of density $n_G = n_G(T, E)$. The two phases are separated by a continuous well-defined interface and related by particle currents between them which only depend on their global properties. The model is then described by means of two connected kinetic cluster-variation equations, one for each homogeneous phase. (4) An alternative mean field approach which locates the critical temperature as the limit of stability of the high T phase. Specifically, one determines the diffusion coefficient by examining the current in response to a small density gradient transverse to the field direction; the vanishing of the diffusion coefficient marks the critical point.

Case 1 has a critical point at $\beta = \infty$ for $J > 0$ (ferromagnetic interactions) at any density and for $J < 0$ (antiferromagnetic interactions) at the critical density $n = \frac{1}{2}$. This is revealed, for instance, by the occurrence there of critical slowing down; when $\beta \neq \infty$, however, the system relaxes exponentially. The steady state properties depend on n, β, E, the sign of J, and the transition rates. We find in particular two qualitatively different behaviors (cf. Figs. 1 and 2): The system with $J < 0$ and $n \neq \frac{1}{2}$, presents similar good conductor states at both low and high temperatures, with a sudden current increase around $T = 4/E$. On the contrary, $J < 0$ at $n = \frac{1}{2}$ and $J > 0$ at any density are characterized by a continuous crossover from an insulator state when $T \ll 4/E$ to a good conductor state when $T > 4/E$, the smooth transition being located, for instance, by a maximum of the specific heat which increases with E (Fig. 4). None of those behaviors is to be associated with the onset of long-ranged order, as noticed before: the qualitative differences are rather a consequence of the degeneracy of the antiferromagnetic ground states when $n < \frac{1}{2}$, a fact which favors large stationary currents at low temperatures. For a given temperature and strength of interactions, the system conductivity is larger for $J < 0$ than for $J > 0$. We also investigated the relation between fluctuations and correlation functions, and find that the behavior of model 1 compares well with the results in some existing, more limited approaches (Fig. 3).

Case 2 shows non-trivial correlations along the two principal axis directions, evidencing, for $\Gamma \to \infty$ and $J > 0$, the existence of anisotropic phase segregation below $T_c(E, n)$. For any given $n < n_c = 0.152$, $T_c(E) < T_c(0)$ decreases monotonically with increasing E, going to zero as $E \to \infty$, while $T_c(E)$ tends asymptotically to a finite value $T_c(\infty)$ for large fields at any given $\frac{1}{2} \geqslant n > n_c$ and $T_c(E, n)$ decreases with n for a given field (cf. Figs. 6 and 7). For $\Gamma \to \infty$ or 0 and $J < 0$, on the contrary, there is no phase transition for any value of E and n, a situation which was already known to occur for $E \to \infty$ and $\Gamma \to \infty$. The phase transition is also suppressed in the limit $\Gamma \to \infty$, independently of the values of E and n, when the interactions are ferromagnetic along the field direction and antiferromagnetic along the horizontal direction, while long-range order is possible when the vertical interactions are repulsive and the horizontal interactions attractive (Fig. 10). When $\Gamma \to 0$ and $J > 0$, $T_c(E)$ decreases monotonically with increasing E, and $T_c(\infty) = 0$,

for all values of n (Figs. 8 and 9). The behavior of this model, and its comparison with the one below, clarifies the role of the parameters E, n, sign of J, and Γ, and describes a changeover from $d = 2$ to $d = 1$.

Case 3 compares well with the MC results (cf. Figs. 11 and 12). In particular, $T_c(E)$ for $J > 0$, $n = \frac{1}{2}$ and $\Gamma = 1$ is an increasing function of E, revealing that the action of the field towards generating strip-like configurations (thus enhancing long-ranged correlations and, consequently, tending to increase T_c), dominates the more local tendency to destroy short-ranged correlations within the strips. The study of the latter, however, uncovers interesting facts concerning critical behavior. The system also reveals the presence of local anisotropic order above $T_c(E)$, a non-equilibrium effect which is known to produce a power law decay of correlations in the high T phase. The slope of the current-versus-temperature curve changes discontinuously at $T_c(E)$. The study of the case $n \neq \frac{1}{2}$ (Figs. 18–21) confirms the MC result that the transition is first order for small values of n. It also follows that states with more than one strip are metastable and not real stationary states, i.e., they will always decay asymptotically towards a single-strip state, though the relaxation time may be large and experimentally observable. Figures 22–25 illustrate further model properties, including the case of varying Γ, which however may lack realism due to a too simple treatment of the interface.

Case 4 allows a precise study of the stability of the high temperature phase. In particular, it yields values for the critical temperatures which are qualitatively similar to and quantitatively close to the MC results.

REFERENCES

1. A. ONUKI AND K. KAWASAKI, *Ann. Phys. (N.Y.)* **131** (1981), 217 and references therein.
2. S. KATZ, J. L. LEBOWITZ, AND H. SPOHN, *Phys. Rev. B* **28** (1983), 1655; *J. Statist. Phys.* **34** (1984), 497.
3. J. MARRO, J. L. LEBOWITZ, H. SPOHN, AND M. K. KALOS, *J. Statist. Phys.* **38** (1985), 725.
4. J. L. VALLÉS AND J. MARRO, *J. Statist. Phys.* **43** (1986), 441.
5. J. L. VALLÉS AND J. MARRO, *J. Statist. Phys.* **49** (1987), 89.
6. J. MARRO AND J. L. VALLÉS, *J. Statist. Phys.* **49** (1987), 121.
7. H. VAN BEIJEREN AND L. S. SCHULMAN, *Phys. Rev. Lett.* **53** (1984), 806.
8. J. KRUG, J. L. LEBOWITZ, H. SPOHN, AND M. Q. ZHANG, *J. Statist. Phys.* **44** (1986), 535.
9. K. LEUNG AND J. L. CARDY, *J. Statist. Phys.* **44** (1986), 567; H. K. JANSSEN AND B. SCHMITTMANN, *Z. Phys. B* **63** (1986), 517.
10. K. GADEWSKI AND A. KUPIAINEN, *Nucl. Phys. B* **269** (1986), 45.
11. R. DICKMAN, *Phys. Rev. A* **38** (1988), 2588.
12. A. DE MASI, P. A. FERRARI, AND J. L. LEBOWITZ, *Phys. Rev. Lett.* **55** (1985), 1947; *J. Statist. Phys.* **44** (1986), 589.
13. J. M. GONZÁLEZ-MIRANDA, P. L. GARRIDO, J. MARRO, AND J. L. LEBOWITZ, *Phys. Rev. Lett.* **59** (1987), 1934.
14. P. L. GARRIDO, J. MARRO, AND J. M. GONZÁLEZ-MIRANDA, *Phys. Rev. A*, submitted; see also J. S. WANG and J. L. LEBOWITZ, *J. Statist. Phys.* **51** (1988), 893.
15. P. L. GARRIDO AND J. MARRO, *J. Statist. Phys.* **49** (1987), 551.
16. P. L. GARRIDO AND J. MARRO, *Physica A* **144** (1987), 585.

17. J. B. BOYCE AND A. B. HUBERMAN, *Phys. Rep.* **51** (1979), 189.
18. M. B. SALAMON (Ed.), "Physics of Superionic Conductors," Springer-Verlag, Berlin, 1979.
19. W. DIETERICH, P. FULDE, AND I. PESCHEL, *Adv. Phys.* **29** (1980), 527.
20. H. U. BEYELER, *in* "Physics in One Dimension" (J. Bernasconi and T. Schneider, Eds.), Springer-Verlag, Berlin, 1981.
21. J. B. BATES, J. WANG, AND N. J. DUBNEY, *Phys. Today*, July (1982), 46.
22. P. BRÜESCH, T. HIBMA, AND W. BÜHRER, *Phys. Rev. B* **27** (1983), 5052.
23. YU. YA. GUVERICH AND YU. KHARKATS, *Phys. Rep.* **139** (1986), 201.
24. R. KIKUCHI, *Phys. Rev.* **81** (1951), 988.
25. R. DICKMAN, *Phys. Rev. A* **34** (1986), 4246.
26. R. DICKMAN, *Phys. Lett. A* **122** (1987), 463.
27. N. METROPOLIS, A. W. ROSENBLUTH, M. M. ROSENBLUTH, A. H. TELLER, AND E. TELLER, *J. Chem. Phys.* **21** (1953), 1087.
28. K. KAWASAKI, *in* "Phase Transitions and Critical Phenomena," Vol. 4 (C. Domb and M. S. Green, Eds.), Academic Press, London, 1972.
29. M. Q. ZHANG, *Phys. Rev. A* **35** (1987), 2266.
30. J. M. ZIMAN, "Models of Disorder," Cambridge Univ. Press, Cambridge, 1979.
31. W. DIETERICH, I. PECHEL, AND W. R. SCHNEIDER, *Commun. Phys.* **2** (1977), 175.
32. H. SATO AND R. KIKUCHI, *J. Chem. Phys.* **55** (1971), 677, 702.
33. R. KIKUCHI, *in* "Fast Ion Transport in Solids" (W. van Gool, Ed.), p. 555, North-Holland, Amsterdam, 1976.
34. P. M. RICHARDS, *Phys. Rev. B* **16** (1977), 1393; **18** (1978), 945.
35. J. BERNASCONI, H. U. BEYELER, S. STRÄSSLER, AND S. ALEXANDER, *Phys. Rev. Lett.* **42** (1979), 819.
36. H. SINGER AND I. PESCHEL, *Z. Phys. B* **39** (1980), 333.
37. H. A. KRAMERS AND G. H. WANNIER, *Phys. Rev.* **60** (1941), 252, 263.
38. N. G. VAN KAMPEN, "Stochastic Processes in Physics and Chemistry," North-Holland, Amsterdam, 1981.
39. cf. Ref. [8, pp. 541–543].
40. J. MARRO, P. L. GARRIDO, A. LABARTA, AND R. TORAL, Critical and finite-size-scaling behavior of short ranged order, *J. Phys.: Condensed Matter*, in press.
41. K.-T. LEUNG, K. K. MON, J. L. VALLÉS, AND R. K. P. ZIA, *Phys. Rev. Lett.* **61** (1988), 1744.
42. M. Q. ZHANG, J. S. WANG, J. L. LEBOWITZ, AND J. L. VALLÉS, *J. Statist. Phys.* **52** (1988), 1461.

Printed by Catherine Press, Ltd., Tempelhof 41, B-8000 Brugge, Belgium